

# Robust Tail Index Estimation under Random Censoring via Minimum Density Power Divergence

Nour Elhouda Guesmia, Abdelhakim Necir\*, Djamel Meraghni

*Laboratory of Applied Mathematics, Mohamed Khider University, Biskra, Algeria*

## Abstract

We propose a robust estimator for the tail index of Pareto-type distributions under random right-censoring, based on the minimum density power divergence (MDPD) framework. To our knowledge, this is the first application of the MDPD approach to extreme value models with random censoring, opening a new direction for robust inference in this setting. Under mild regularity conditions, the estimator is shown to be consistent and asymptotically normal. Its performance in finite samples is extensively evaluated through simulation studies, demonstrating superior robustness and efficiency compared to existing methods. Contamination is introduced only before censoring to provide a meaningful assessment of robustness, while contamination after censoring is shown to yield distorted or unrealistic results. The practical relevance of the approach is illustrated using a real dataset on insurance claims, which features light censoring and fully observable extremes, and a dataset on AIDS survival times, which, despite stronger censoring ( $p < 1/2$ ), allows for illustrative comparisons and highlights practical limitations and challenges in more difficult scenarios.

**Keywords:** Asymptotic normality; Heavy-tails; Robust estimation; Random right-censoring; Tail index.

**AMS 2020 Subject Classification:** 62G32; 62G05; 62G20; 62G35.

\*Corresponding author: ah.necir@univ-biskra.dz

*E-mail address:*

nourelhouda.guesmia@univ-biskra.dz (N. Guesmia)

djamel.meraghni@univ-biskra.dz (D. Meraghni)

## 1. Introduction

Right-censored data pose a common challenge in statistics, as values are only known up to a certain threshold, while those beyond it remain unobserved. This situation frequently arises in fields such as survival analysis, reliability engineering, and insurance. Pareto-type distributions are commonly used to model data exhibiting extreme values. These distributions are characterized by a relatively high probability of producing observations far from the mean, in contrast with the normal distribution. They are particularly relevant in applications such as insurance, finance, and environmental studies, where rare events can have a substantial impact.

Let  $X_1, X_2, \dots, X_n$  be a sample of size  $n \geq 1$  from a random variable (rv)  $X$ , and let  $C_1, C_2, \dots, C_n$  be another sample from a rv  $C$ , both defined on a probability space  $(\Omega, \mathcal{A}, \mathbf{P})$ , with continuous cumulative distribution functions (cdfs)  $F$  and  $G$ , respectively. Assume that  $X$  and  $C$  are independent. We also suppose that  $X$  is right censored by  $C$ , meaning that for each index  $1 \leq j \leq n$ , we can only observe the variable

$$Z_j := \min \{X_j, C_j\}$$

and the indicator variable

$$\delta_j := \mathbb{I}_{\{X_j \leq C_j\}},$$

which determines whether or not  $X$  has been observed. We assume that the tail functions  $\bar{F} := 1 - F$  and  $\bar{G} := 1 - G$  are regularly varying at infinity (or Pareto-type) of positive tail indices  $\gamma_1 > 0$  and  $\gamma_2 > 0$ , allowing for slowly varying deviations from the strict Pareto form. More precisely, for any  $x > 0$ ,

$$\lim_{u \rightarrow \infty} \frac{\bar{F}(ux)}{\bar{F}(u)} = x^{-1/\gamma_1} \text{ and } \lim_{u \rightarrow \infty} \frac{\bar{G}(ux)}{\bar{G}(u)} = x^{-1/\gamma_2}. \quad (1.1)$$

Equivalently, these tail behaviors can be expressed in terms of slowly varying functions  $\ell_1(x)$  and  $\ell_2(x)$  to account for deviations from strict Pareto distributions:

$$\bar{F}(x) = x^{-1/\gamma_1} \ell_1(x) \text{ and } \bar{G}(x) = x^{-1/\gamma_2} \ell_2(x), \quad (1.2)$$

where  $\ell_1(x)$  and  $\ell_2(x)$  vary slowly at infinity, i.e., for any fixed  $t > 0$ ,

$$\ell_j(tx) / \ell_j(x) \rightarrow 1, \text{ as } x \rightarrow \infty, \quad j = 1, 2.$$

These expressions make explicit the Pareto-type form of the distributions and clarify that the limit relations correspond to first-order asymptotics, while the slowly varying functions explicitly capture deviations from a strict Pareto model.

We denote the cdf of  $Z$  by  $H$ . Then, using the independence of  $X$  and  $C$ , we have

$$\bar{H} = \bar{F} \times \bar{G},$$

which implies that  $\bar{H}$  is also regularly varying at infinity, with tail index

$$\gamma := \frac{\gamma_1 \gamma_2}{\gamma_1 + \gamma_2}.$$

This characterization of the tail behavior of the observed variable  $Z$  provides a firm basis for estimating the tail index  $\gamma$  under right censoring. In the subsequent sections, we develop estimation procedures that appropriately account for censored observations and examine their asymptotic properties, including robustness to contamination.

In the presence of extreme values and right-censored data, various methods have been proposed for estimating the tail index. Several techniques have been developed to address the specific challenges posed by such data. Many studies have focused on modifying traditional tail index estimation methods, notably Hill's estimator (Hill, 1975) to accommodate censored observations. In particular, Einmahl *et al.* (2008) adapted this estimator to handle right-censored data, leading to the following form:

$$\hat{\gamma}_1^{(EFG)} := \frac{\hat{\gamma}^{(H)}}{\hat{p}},$$

where

$$\hat{\gamma}^{(H)} := k^{-1} \sum_{i=1}^k \log (Z_{n-i+1:n} / Z_{n-k:n}),$$

denotes the classical Hill estimator corresponding to the tail index  $\gamma$ , and

$$\hat{p} := k^{-1} \sum_{i=1}^k \delta_{[n-i+1:n]},$$

represents an estimator of the proportion of upper non-censored observations,

$$p := \frac{\gamma_2}{\gamma_1 + \gamma_2}. \quad (1.3)$$

The integer sequence  $k = k_n$  represents the number of top order statistics used in the estimation of the tail index so that  $k \rightarrow \infty$  and  $k/n \rightarrow 0$  as  $n \rightarrow \infty$ . This ensures that enough extreme observations are included for reliable estimation, while avoiding the inclusion of too many moderate values that could bias the tail index estimate.

The sequence of rvs  $Z_{1:n} \leq \dots \leq Z_{n:n}$  represents the order statistics pertaining to the sample  $Z_1, \dots, Z_n$  and  $\delta_{[1:n]}, \dots, \delta_{[n:n]}$  denotes the corresponding concomitant values, satisfying  $\delta_{[j:n]} = \delta_i$  for  $i$  such that  $Z_{j:n} = Z_i$ . This notation clarifies the alignment between the ordered observations and their censoring indicators, which is essential for constructing the censored Hill-type estimator.

On the basis of a Kaplan-Meier integration, [Worms and Worms \(2014\)](#) proposed a consistent estimator to the tail index  $\gamma_1$  defined by

$$\hat{\gamma}_1^{(W)} := \sum_{i=1}^k \frac{\bar{F}_n^{(KM)}(Z_{n-i:n})}{\bar{F}_n^{(KM)}(Z_{n-k:n})} \log \frac{Z_{n-i+1:n}}{Z_{n-i:n}},$$

where

$$F_n^{(KM)}(x) := 1 - \prod_{Z_{i:n} \leq x} \left( \frac{n-i}{n-i+1} \right)^{\delta_{[i:n]}},$$

denotes the popular Kaplan-Meier estimator of cdf  $F$  ([Kaplan and Meier, 1958](#)). The asymptotic normality of  $\hat{\gamma}_1^{(W)}$  is established in [Beirlant et al. \(2019\)](#) by considering Hall's model ([Hall, 1982](#)). Bias reduction in tail index estimation under censoring has been addressed in [Beirlant et al. \(2016\)](#), [Beirlant et al. \(2018\)](#) and [Beirlant et al. \(2019\)](#).

By using a Nelson-Aalen integration, recently [Meraghni et al. \(2025\)](#) derived a new estimator for  $\gamma_1$  given by

$$\hat{\gamma}_1^{(MNS)} := \sum_{i=1}^k \frac{\delta_{[n-i+1:n]}}{i} \frac{\bar{F}_n^{(NA)}(Z_{n-i+1:n})}{\bar{F}_n^{(NA)}(Z_{n-k:n})} \log \frac{Z_{n-i+1:n}}{Z_{n-k:n}},$$

where

$$F_n^{(NA)}(x) = 1 - \prod_{Z_{i:n} < x} \exp \left\{ -\frac{\delta_{[i:n]}}{n-i+1} \right\}, \quad (1.4)$$

denotes the well-known Nelson-Aalen estimator of cdf  $F$  ([Nelson, 1972](#)). Note that

$$\frac{\bar{F}_n^{(NA)}(Z_{n-i+1:n})}{\bar{F}_n^{(NA)}(Z_{n-k:n})} = \prod_{j=i+1}^k \exp \left\{ -\frac{\delta_{[n-j+1:n]}}{j} \right\}, \quad (1.5)$$

thus the formula of  $\hat{\gamma}_1^{(MNS)}$  can be rewritten as

$$\hat{\gamma}_1^{(MNS)} := \sum_{i=1}^k a_{ik} \log \frac{Z_{n-i+1:n}}{Z_{n-k:n}},$$

where

$$a_{ik} := \frac{\delta_{[n-i+1:n]}}{i} \prod_{j=i+1}^k \exp \left\{ -\frac{\delta_{[n-j+1:n]}}{j} \right\}. \quad (1.6)$$

This representation highlights the connection between the Nelson-Aalen weights  $a_{ik}$  and the Kaplan-Meier-based integration, and makes explicit the recursive weighting scheme that adjusts for censoring in the upper tail.

The asymptotic properties of both the Kaplan-Meier-based estimator  $\hat{\gamma}_1^{(W)}$  and the Nelson-Aalen-based estimator  $\hat{\gamma}_1^{(MNS)}$  are established provided that  $p > 1/2$ . This condition ensures that a sufficiently large fraction of extreme observations remains uncensored, which is essential for reliable estimation of  $\gamma_1$ . Equivalently, it can be expressed as  $\gamma_1 < \gamma_2$ , meaning that the censoring distribution has a lighter tail than the distribution of interest. If  $p \leq 1/2$  (or  $\gamma_1 \geq \gamma_2$ ), the effective tail sample size may be too small, and the Gaussian approximation

underlying these estimators may break down. In practice, this condition serves as a natural guideline for the applicability of both estimators, emphasizing the importance of the relative tail heaviness between the observed and censoring distributions.

The authors showed that the two tail index estimators  $\hat{\gamma}_1^{(W)}$  and  $\hat{\gamma}_1^{(MNS)}$  exhibit similar performances in terms both of bias and mean squared error (MSE). Indeed, studies comparing the Kaplan–Meier and Nelson–Aalen estimators have shown that the latter exhibits an almost identical statistical behavior; see, for instance, [Colosimo et al. \(2002\)](#). On the other hand, establishing the asymptotic properties of extreme Kaplan–Meier integrals poses certain technical difficulties. To overcome this issue, [Meraghni et al. \(2025\)](#) introduced a Nelson–Aalen tail-product limit process and established its Gaussian approximation in terms of standard Wiener processes. Using this approach, they proved the consistency and asymptotic normality of the proposed estimator  $\hat{\gamma}_1^{(MNS)}$  under the first- and second-order regular variation conditions, namely the assumptions (1.1) and (3.13) respectively. As expected, it was also shown that both the asymptotic bias and variance of  $\hat{\gamma}_1^{(W)}$  and  $\hat{\gamma}_1^{(MNS)}$  are equal, highlighting the practical equivalence of the two estimators under the stated assumptions.

The most common method for estimating the parameters of an extreme value distribution in extreme value analysis relies on the maximum likelihood estimation (MLE) method. Although these estimators possess desirable asymptotic properties, they can be sensitive to outlying observations from the assumed extreme value models; see, for instance, [Brazauskas and Serfling \(2000\)](#). Consequently, robust statistical methods provide a better alternative to mitigate the influence of outliers and deviations from the underlying parametric models. It has been shown that employing robust statistical ideas in extreme value theory improves the quality and precision of estimates ([Dell'Aquila and Embrechts, 2006](#)).

[Juárez and Schucany \(2004\)](#) appear to be the first authors to employ the minimum density power divergence (MDPD) of [Basu et al. \(1998\)](#) for the robust estimation of the parameters of an extreme value distribution. Since then, this divergence measure has become a widely used tool for robust estimation of parameters of extreme value distributions. [Kim and Lee \(2008\)](#), [Dierchx et al. \(2013\)](#), [Goegebeur et al. \(2014\)](#), [Dierckx et al. \(2021\)](#) have applied the MDPD approach to estimate the tail index and quantiles from Pareto-type distributions. Recently, [Ghosh \(2017\)](#) proposed a robust MDPD estimator for a real-valued tail index. This estimator is a robust generalization of the estimator proposed by [Matty and Beirlant \(2003\)](#) and addresses non-identical distributions in the exponential regression model using the approach in [Ghosh and Basu \(2013\)](#). Furthermore, [Dierchx et al. \(2013\)](#) employed the MDPD concept on an extended Pareto distribution for relative excesses over a high threshold. [Minkah et al. \(2023A\)](#) and [Minkah et al. \(2023B\)](#) recently proposed a robust estimator for the

tail index of a Pareto-type distribution using the MDPD approach applied to an exponential regression model.

While robust estimation techniques have been extensively developed for complete data settings, their extension to the context of randomly right-censored observations remains comparatively less explored. Such censoring mechanisms are prevalent in survival analysis, reliability theory, and actuarial applications, where incomplete information introduces additional statistical challenges. Classical estimators of the extreme value index under censoring, such as Hill-type approaches or those based on Kaplan-Meier and Nelson-Aalen integrals, often remain sensitive to outliers and model deviations, thereby limiting their practical robustness in real-world applications.

To the best of our knowledge, apart from the recent work of [Dierckx \*et al.\* \(2021\)](#), there exists no robust estimator specifically tailored for the tail index under random censoring. Their approach focuses on the conditional tail index, employing kernel smoothing techniques and local threshold selection for each covariate value. While the estimator effectively reduces bias and variance in the presence of contamination, it relies on a separate selection of tuning parameters and is restricted to the conditional setting, which complicates its direct application to the unconditional tail index. This limitation underscores the need for a robust and flexible framework capable of handling both unconditional and censored extreme value scenarios, motivating the development of the MDPD-based estimator proposed in this work.

The remainder of this paper is organized as follows. Section 2 provides a brief overview of the MDPD estimation method, originally introduced by [Basu \*et al.\* \(1998\)](#), highlighting its robust properties in the presence of outliers. Section 3 discusses in detail the asymptotic properties (consistency and asymptotic normality) of the proposed estimator, with full proofs deferred to Section 7. The finite-sample performance of the estimator is examined in Section 4, through a comprehensive simulation study, including comparisons with existing tail index estimators under censoring and contamination. Section 5 presents real-data applications, including a dataset on insurance claims (where censoring is relatively light,  $p > 1/2$ ) and the classical AIDS survival dataset, illustrating the practical relevance and robustness of the proposed methodology.

Finally, Appendix A compiles several technical lemmas and propositions that are instrumental to the theoretical development, while Appendix B contains the figures and additional results related to the simulation study.

## 2. Minimum density power divergence

Basu *et al.* (1998) introduced a new measure of divergence between two probability densities  $\ell$  and  $f$ , known as the density power divergence (DPD), by

$$d_\alpha(f, \ell) := \begin{cases} \int_{\mathbb{R}} \left[ \ell^{1+\alpha}(x) - \left(1 + \frac{1}{\alpha}\right) \ell^\alpha(x) f(x) + \frac{1}{\alpha} f^{1+\alpha}(x) \right] dx, & \alpha > 0 \\ \int_{\mathbb{R}} f(x) \log \frac{f(x)}{\ell(x)} dx, & \alpha = 0, \end{cases} \quad (2.7)$$

where  $\alpha \geq 0$  is a tuning parameter controlling the trade-off between efficiency and robustness. The case  $\alpha = 0$  is the limit of the general expression ( $\alpha > 0$ ) as  $\alpha \downarrow 0$  yielding the classical Kullback-Leibler divergence  $d_0(f, \ell)$ . Let us consider a parametric family of densities  $\{\ell_\theta : \Theta \subset \mathbb{R}^p\}$  and suppose that the goal is to estimate the parameter  $\theta$ . Let  $F$  denote the cdf corresponding to the density  $f$ . The MDPD functional  $T_\alpha(F)$  is defined as

$$d_\alpha(f, \ell_{T_\alpha(F)}) = \min_{\theta \in \Theta} d_\alpha(f, \ell_\theta).$$

The term  $\int f^{1+\alpha}(x) dx$  in (2.7) the divergence does not depend on  $\theta$ , and thus does not affect the minimization. Therefore, minimizing  $d_\alpha(f, \ell_\theta)$  over  $\theta \in \Theta$  reduces to minimizing

$$\delta_\alpha(f; \theta) := \begin{cases} \int_{\mathbb{R}} \ell_\theta^{1+\alpha}(x) dx - \left(1 + \frac{1}{\alpha}\right) \int_{\mathbb{R}} \ell_\theta^\alpha(x) dF(x), & \alpha > 0, \\ - \int_{\mathbb{R}} \log \ell_\theta(x) dF(x), & \alpha = 0. \end{cases}$$

Given a sample  $X_1, \dots, X_n$  from the cdf  $F$ , we estimate  $\delta_\alpha(f; \theta)$  by replacing  $F$  with its empirical counterpart  $F_n(x) := n^{-1} \sum_{i=1}^n \mathbb{I}_{\{X_i \leq x\}}$ . The MDPD estimator is then the minimizer (over  $\theta \in \Theta$ ) of the empirical objective function

$$L_{n,\alpha}(\theta) = \begin{cases} \int_{\mathbb{R}} \ell_\theta^{1+\alpha}(x) dx - \left(1 + \frac{1}{\alpha}\right) \frac{1}{n} \sum_{i=1}^n \ell_\theta^\alpha(X_i), & \alpha > 0, \\ -\frac{1}{n} \sum_{i=1}^n \log \ell_\theta(X_i), & \alpha = 0. \end{cases}.$$

That is,  $\hat{\theta}_{n,\alpha} := \arg \min_{\theta \in \Theta} L_{n,\alpha}(\theta)$ , which satisfies the estimating equation

$$\begin{cases} \int_{\mathbb{R}} \frac{d}{d\theta} \ell_\theta^{1+\alpha}(x) dx - \left(1 + \frac{1}{\alpha}\right) \frac{1}{n} \sum_{i=1}^n \frac{d}{d\theta} \ell_\theta^\alpha(X_i) = 0, & \alpha > 0, \\ \frac{1}{n} \sum_{i=1}^n \frac{d}{d\theta} \log \ell_\theta(X_i) = 0, & \alpha = 0. \end{cases}$$

Small  $\alpha$  yields high efficiency with limited robustness, while moderate  $\alpha$  values provide strong robustness under contamination with minor efficiency loss compared to MLE under correct model specification.

**2.1. MDPD estimator of  $\gamma_1$  for right-censored data.** For a fixed threshold  $u > 0$ , consider the relative excess rv  $Y := X/u$  conditional on  $X > u$ . Its cdf is given by

$$F_u(x) := 1 - \frac{\bar{F}(ux)}{\bar{F}(u)},$$

with corresponding probability density function  $f_u$ . Assuming that  $\bar{F} \in \mathcal{RV}_{(-1/\gamma_1)}$ , it follows that  $F_u(x) \approx 1 - x^{-1/\gamma_1}$ , as  $u \rightarrow \infty$ . Therefore, the rv  $Y$  may be approximated by the Pareto distribution with density

$$\ell_{\gamma_1}(x) := \frac{d}{dx} (1 - x^{-1/\gamma_1}) = \gamma_1^{-1} x^{-1-1/\gamma_1}, \text{ for } x \geq 1.$$

The corresponding DPD objective function is

$$\mathcal{L}_{u,\alpha}^*(\gamma_1) := \begin{cases} \int_1^\infty \ell_{\gamma_1}^{1+\alpha}(x) dx - \left(1 + \frac{1}{\alpha}\right) \int_u^\infty \ell_{\gamma_1}^\alpha(x/u) d\frac{F(x)}{\bar{F}(u)}, & \alpha > 0, \\ \int_u^\infty \log \ell_{\gamma_1}(x/u) d\frac{F(x)}{\bar{F}(u)}, & \alpha = 0, \end{cases} \quad (2.8)$$

Letting  $u = Z_{n-k:n}$  and replacing  $F$  with the Nelson-Aalen estimator  $F_n^{(NA)}$  gives the empirical objective function

$$\mathcal{L}_{k,\alpha}^*(\gamma_1) := \begin{cases} \int_1^\infty \ell_{\gamma_1}^{1+\alpha}(x) dx - \left(1 + \frac{1}{\alpha}\right) \int_1^\infty \ell_{\gamma_1}^\alpha(x/Z_{n-k:n}) d\frac{F_n^{(NA)}(x)}{\bar{F}_n^{(NA)}(Z_{n-k:n})}, & \alpha > 0, \\ \int_1^\infty \log \ell_{\gamma_1}(x/Z_{n-k:n}) d\frac{F_n^{(NA)}(x)}{\bar{F}_n^{(NA)}(Z_{n-k:n})}, & \alpha = 0. \end{cases} \quad (2.9)$$

The MDPD tail index estimator under random censoring, denoted  $\hat{\gamma}_{1,\alpha}$ , is then obtained by minimizing  $\mathcal{L}_{k,\alpha}^*(\gamma_1)$ . That is, by solving the following equation:

$$\begin{cases} \int_1^\infty \frac{d}{d\gamma_1} \ell_{\gamma_1}^{1+\alpha} \left( \frac{x}{Z_{n-k:n}} \right) dx \\ \quad - \left(1 + \frac{1}{\alpha}\right) \int_1^\infty \frac{d}{d\gamma_1} \ell_{\gamma_1}^\alpha \left( \frac{x}{Z_{n-k:n}} \right) d\frac{F_n^{(NA)}(x)}{\bar{F}_n^{(NA)}(Z_{n-k:n})} = 0, & \alpha > 0, \\ \int_1^\infty \frac{d}{d\gamma_1} \log \ell_{\gamma_1} \left( \frac{x}{Z_{n-k:n}} \right) d\frac{F_n^{(NA)}(x)}{\bar{F}_n^{(NA)}(Z_{n-k:n})} = 0, & \alpha = 0. \end{cases}$$

By elementary calculations:

$$\frac{d}{d\gamma_1} \ell_{\gamma_1}^\alpha(x) = \frac{\alpha}{\gamma_1^{2+\alpha}} \frac{\log x - \gamma_1}{x^{\alpha(1+1/\gamma_1)}},$$

$$\frac{d}{d\gamma_1} \log \ell_{\gamma_1}(x) = \frac{d}{d\gamma_1} \log (\gamma_1^{-1} x^{-1-1/\gamma_1}) = -\frac{\gamma_1 - \log x}{\gamma_1^2}$$

and

$$\int_1^\infty \frac{d}{d\gamma_1} \ell_{\gamma_1}^{1+\alpha}(x) dx = -\frac{\alpha(\alpha+1)(\gamma_1+1)}{\gamma_1^{\alpha+1}(\alpha(1+\gamma_1)+1)^2}.$$

Hence, the estimating equation for  $\hat{\gamma}_{1,\alpha}$  is

$$\begin{cases} \int_{Z_{n-k:n}}^{\infty} \frac{\gamma_1 - \log(x/Z_{n-k:n})}{(x/Z_{n-k:n})^{\alpha(1+1/\gamma_1)}} d\frac{F_n^{(NA)}(x)}{\bar{F}_n^{(NA)}(Z_{n-k:n})} = \frac{\alpha\gamma_1(\gamma_1+1)}{(1+\alpha+\alpha\gamma_1)^2}, & \alpha > 0, \\ \int_{Z_{n-k:n}}^{\infty} \left( \gamma_1 - \log \frac{x}{Z_{n-k:n}} \right) d\frac{F_n^{(NA)}(x)}{\bar{F}_n^{(NA)}(Z_{n-k:n})} = 0, & \alpha = 0. \end{cases} \quad (2.10)$$

Meraghni *et al.* (2025) stated that

$$dF_n^{(NA)}(x) = \frac{\bar{F}_n^{(NA)}(x) dH_n^{(1)}(x)}{\bar{H}_n(x^-)}, \quad (2.11)$$

where  $H_n$  and  $H_n^{(1)}$  are the empirical counterparts of the cdf  $H$  and the sub-distribution  $H^{(1)}$ , respectively defined by:

$$H_n(x) := \frac{1}{n} \sum_{i=1}^n \mathbb{I}_{\{Z_{i:n} \leq x\}} \text{ and } H_n^{(1)}(x) := \frac{1}{n} \sum_{i=1}^n \delta_{[i:n]} \mathbb{I}_{\{Z_{i:n} \leq x\}},$$

(see, for example, Shorack and Wellner (1986) page 294). Here,  $f(x^-)$  denotes the left limit, at  $x$ , of the function  $f$ . By substituting  $dF_n^{(NA)}(x)$  with its expression in equation (2.10), we get

$$\begin{cases} \sum_{i=1}^k a_{ik} \frac{\gamma_1 - \log(Z_{n-i+1:n}/Z_{n-k:n})}{(Z_{n-i+1:n}/Z_{n-k:n})^{\alpha(1+1/\gamma_1)}} = \frac{\alpha\gamma_1(\gamma_1+1)}{(1+\alpha+\alpha\gamma_1)^2}, & \alpha > 0, \\ \sum_{i=1}^k a_{ik} \left\{ \gamma_1 - \log \frac{Z_{n-i+1:n}}{Z_{n-k:n}} \right\} = 0, & \alpha = 0, \end{cases} \quad (2.12)$$

where  $a_{ik}$  are the Nelson-Aalen weights defined, earlier, in (1.6).

This estimator provides the first robust generalization of the tail index under random censoring using the MDPD approach, bridging the gap between efficiency and robustness in extreme value estimation.

### 3. Consistency and asymptotic normality

From now on, we denote the true value of  $\gamma_1$  by  $\gamma_1^*$ .

**Theorem 3.1.** (*Consistency*) Assume that the cdfs  $F$  and  $G$  satisfy the first-order regular variation condition (1.1) and that  $p > 1/2$ . Let  $k = k_n$  be a sequence of integers such that

$$k \rightarrow \infty \text{ and } k/n \rightarrow 0, \text{ as } n \rightarrow \infty.$$

Then, for any  $\alpha > 0$ , with probability tending to 1, there exists a solution  $\hat{\gamma}_{1,\alpha}$  to the estimating equation (2.12) such that

$$\hat{\gamma}_{1,\alpha} \xrightarrow{\mathbf{P}} \gamma_1^*, \text{ as } n \rightarrow \infty.$$

This result establishes the consistency of the MDPD tail index estimator under random censoring, underlining that a sufficient proportion of uncensored extreme observations ( $p > 1/2$ ) is crucial for reliable estimation.

Since weak approximations of extreme value theory-based statistics are typically achieved within the second-order framework (see, i.e., [de Haan and Stadtmüller, 1996](#)), we assume that the cdf  $F$  satisfies the well-known second-order condition of regular variation. Specifically, for any  $x > 0$  :

$$\lim_{t \rightarrow \infty} \frac{U_F(tx)/U_F(t) - x^{\gamma_1}}{A_1^*(t)} = x^{\gamma_1} \frac{x^{\tau_1} - 1}{\tau_1}, \quad (3.13)$$

where  $\tau_1 \leq 0$  is the second-order parameter, and  $A_1^*$  is a function tending to 0, not changing sign near infinity and whose absolute value is regularly varying with index  $\tau_1$ . When  $\tau_1 = 0$ , the expression  $(x^{\tau_1} - 1)/\tau_1$  is interpreted as  $\log x$ .

We denote the quantile and tail quantile functions of a given cdf  $D$  by

$$\mathcal{D}^\leftarrow(s) := \inf \{x : \mathcal{D}(x) \geq s\}, \quad 0 < s < 1$$

and

$$U_{\mathcal{D}}(t) := \mathcal{D}^\leftarrow(1 - 1/t), \quad t > 1,$$

respectively.

For convenience, we set  $h := U_H(n/k)$  and define  $A_1(t) := A_1^*(1/\bar{F}(t))$ , for  $t > 1$ .

**Theorem 3.2.** *(Asymptotic normality) Assume that the cdfs  $F$  and  $G$  satisfy the second-order condition (3.13) and that  $p > 1/2$ . Let  $k = k_n$  be a sequence of integers such that*

$$k \rightarrow \infty, \quad k/n \rightarrow 0 \quad \text{and} \quad \sqrt{k}A_1(h) \rightarrow \lambda < \infty, \quad \text{as } n \rightarrow \infty.$$

*Then for any  $\alpha > 0$  :*

$$\left(1 + \frac{1}{\alpha}\right)^{-1} \eta^* \sqrt{k}(\hat{\gamma}_{1,\alpha} - \gamma_1^*) \xrightarrow{\mathcal{D}} \mathcal{N}(\lambda\mu, \sigma^2), \quad \text{as } n \rightarrow \infty,$$

*where  $\eta^*$ ,  $\mu$  and  $\sigma^2$  are defined in (8.27), (7.21) and (8.28), respectively.*

This theorem establishes the asymptotic normality of the MDPD estimator under random censoring, emphasizing again that the condition  $p > 1/2$  is essential for the validity of the Gaussian approximation.

#### 4. SIMULATION STUDY

In this section, we investigate the finite-sample performance of the proposed MDPD tail index estimator  $\hat{\gamma}_{1,\alpha}$  through an extensive Monte Carlo simulation study. The main objective is to assess both efficiency and robustness under random right censoring and contamination affecting the upper tail.

More specifically, the simulation design is intended to highlight the trade-off between efficiency and robustness induced by the tuning parameter  $\alpha$  across a wide range of realistic and adverse configurations.

**4.1. Data-generating mechanism.** We consider two heavy-tailed distributions for the latent variable  $X$  :

- **Burr distribution:**  $F(x) = 1 - (1+x^{1/\eta})^{-\eta/\gamma_1}$ ,  $x > 0$ , with shape parameter  $\eta = 0.25$  and tail index  $\gamma_1 \in \{0.3, 0.5\}$ .
- **Fréchet distribution:**  $F(x) = \exp(-x^{-1/\gamma_1})$ ,  $x > 0$ , with tail index  $\gamma_1 \in \{0.3, 0.5\}$ .

Right censoring is generated independently via a rv  $C$  from the same parametric family as  $F$  with censoring tail index  $\gamma_2$ , such that the proportion of uncensored extreme observations  $p > 1/2$ . This ensures that the observed rv  $Z = \min(X, C)$  remains regularly varying and satisfies the weak censoring condition discussed in Section 1.

This construction guarantees a controlled censoring mechanism while preserving the asymptotic tail behavior of the observed data.

**4.2. Contamination schemes.** To evaluate robustness, three contamination scenarios are considered, reflecting increasing levels of difficulty and realism.

(1) **Original (uncontaminated) data:**

The latent rvs  $X_i$  are generated from the target cdf  $F$ , and the observed pairs  $(Z_i, \delta_i)$  through the censoring mechanism. This setting provides a baseline for assessing efficiency under the correctly specified model.

(2) **Contamination before censoring:**

A fraction  $\epsilon$  of the latent rvs  $X_i$  is replaced by extreme values drawn from a Burr distribution  $F_c$  with a heavier tail than the target cdf  $F$ . The censoring mechanism is then applied to the contaminated latent sample, yielding the observed data

$$(Z_i^{(\epsilon)}, \delta_i^{(\epsilon)}) := \left( \min(X_i^{(\epsilon)}, C_i), \mathbb{I}_{\{X_i^{(\epsilon)} \leq C_i\}} \right), \quad i = 1, \dots, n.$$

This scenario corresponds to a classical robustness framework in which contamination directly affects the true underlying distribution  $F$ . The Burr distribution is chosen as a flexible heavy-tailed contaminating model, ensuring a pronounced impact

on the upper tail while allowing precise control of tail heaviness. Although other heavy-tailed distributions could be considered, the Burr family provides a convenient parametrization and has been widely used in extreme value simulation studies. This setting serves as a benchmark for evaluating robustness when contamination acts at the latent level and is partially filtered by the censoring mechanism.

(3) **Contamination after censoring:** only the observed pairs  $(Z_i, \delta_i)$  are available. Pseudo-samples  $(\tilde{X}_i)$  are first generated from the Kaplan–Meier estimator  $F_n^{(KM)}$  using the inversion method, and contamination is applied to  $(\tilde{X}_i)$ . The observed data are then reconstructed as

$$(\tilde{Z}_i^{(\epsilon)}, \tilde{\delta}_i^{(\epsilon)}) := \left( \min(\tilde{X}_i^{(\epsilon)}, C_i), \mathbb{I}_{\{\tilde{X}_i^{(\epsilon)} \leq C_i\}} \right), \quad i = 1, \dots, n.$$

This approach provides an illustrative robustness assessment in situations where contamination directly affects the observed extremes, rather than the latent variable itself. It reflects a realistic and particularly adverse scenario encountered in practice, where outliers may arise from data recording errors, reporting issues, or abnormal external events occurring after censoring has taken place.

**4.3. Generation of pseudo-samples from the Kaplan–Meier estimator.** When the latent variables  $X_i$  are unobserved due to right censoring, pseudo-observations can be generated from the Kaplan–Meier estimator  $F_n^{(KM)}$ , constructed on the basis of the observed pairs  $(Z_i, \delta_i)$ , using the inversion method.

Formally, let  $U_i, i = 1, \dots, n$ , be independent rvs uniformly distributed on  $(0, 1)$ , defined on the probability space  $(\Omega, \mathcal{A}, \mathbf{P})$ . We define the pseudo-observations by

$$\tilde{X}_i = Q_n^{(KM)}(U_i),$$

where

$$Q_n^{(KM)}(s) := \min \{x \in \mathbb{R} : F_n^{(KM)}(x) \geq s\}, \quad 0 < s < 1,$$

denotes the empirical quantile function associated with  $F_n^{(KM)}$ .

The resulting pseudo-sample can be interpreted as a sample drawn from an estimate of the latent distribution function  $F$ , reconstructed from the censored data. This approach provides a principled way to approximate the underlying distribution while fully accounting for the censoring mechanism, and allows contamination to be introduced in a manner consistent with the information actually available to the statistician. As a consequence, the contamination mechanism remains coherent with the observed-data structure, which is essential for a meaningful robustness analysis.

**4.4. Simulation scenarios and settings.** Although infinitely many combinations of target, censoring, and contamination distributions could be considered, we restrict our attention to two representative scenarios that are commonly used in extreme value analysis and that allow for a clear and informative assessment of both efficiency and robustness.

The following scenarios are implemented:

- **S1:** Burr/Burr/Burr: the target variable  $X$  follows Burr distribution, the censoring variable is also Burr-distributed, and contamination is introduced via a Burr distribution with parameters  $\eta_c = 0.25$  and  $\gamma_c = \{0.6, 0.8\}$ .
- **S2:** Fréchet/Fréchet/Fréchet: the target variable  $X$  follows a Fréchet distribution, the censoring mechanism is Fréchet-distributed, and contamination is generated from a Fréchet distribution with tail index  $\gamma_c = \{0.6, 0.8\}$ .

The MDPD estimator  $\widehat{\gamma}_{1,\alpha}$  is computed for  $\alpha \in \{0.1, 0.3, 0.5\}$ . For comparison, we include the following benchmark estimators:

- Adapted Hill-type  $\widehat{\gamma}_1^{(EFG)}$ ,
- Kaplan–Meier-based  $\widehat{\gamma}_1^{(W)}$ ,
- Nelson–Aalen-based  $\widehat{\gamma}_1^{(MNS)}$  (for  $\alpha = 0$ ).

This selection covers both classical and censoring-adapted tail index estimators that are widely used in the literature.

**4.5. Selection of the number of upper order statistics.** The number of upper order statistics  $k$  is selected using the adaptive algorithm of Reiss and Thomas [Reiss and Thomas \(2007\)](#), which aims at stabilizing tail index estimation based on uncensored extremes. Specifically, the optimal value  $k^*$  is defined as

$$k^* := \arg \min_{1 < k < n} \frac{1}{k} \sum_{i=1}^k i^\theta \left| \widehat{\zeta}_i - \text{median}(\widehat{\zeta}_1, \dots, \widehat{\zeta}_k) \right|, \quad 0 \leq \theta \leq 0.5,$$

where  $\widehat{\zeta}_i$  denotes an estimator of the tail parameter  $\eta$  computed from the  $i$  largest order statistics. Throughout this work, we fix  $\theta = 0.3$ .

This choice is supported by an extensive empirical calibration based on a preliminary study of  $\theta$  over the interval  $[0, 0.5]$ , which systematically examined the sensitivity of the procedure to the tuning parameter and showed that  $\theta = 0.3$  consistently provides a favorable compromise in terms of bias and mean squared error across the considered scenarios. Smaller values of  $\theta$  tend to oversmooth the variability among the upper order statistics, thereby masking relevant tail information, whereas larger values overemphasize extreme fluctuations, resulting in increased variance and reduced numerical stability.

Thus, fixing  $\theta = 0.3$  offers a stable and numerically well-justified balance between robustness and sensitivity to extremes. This value was found to perform reliably across different tail indices, censoring levels, and contamination regimes. The Reiss–Thomas selection procedure is applied uniformly throughout the simulation study, thereby ensuring a fair comparison between the different estimators. Further details on this selection rule can be found in [Neves and Fraga Alves \(2004\)](#).

**4.6. Performance evaluation.** Absolute bias (Bias) and mean squared error (MSE) are computed over a large number of Monte Carlo replications, providing a reliable assessment of the finite-sample behavior of the estimators.

Graphical representations are used to illustrate the combined effects of contamination, censoring, and the robustness parameter  $\alpha$  on tail index estimation accuracy, with particular emphasis on stability with respect to the number of upper order statistics.

**4.7. Simulation Results.** This section is organized into two complementary parts. We first examine the behavior of the proposed estimator when contamination affects the latent data prior to the censoring mechanism. We then consider a more realistic setting in which contamination is introduced after censoring, when only censored observations are available. This structure allows for a direct and transparent comparison between two fundamentally different contamination mechanisms.

**4.7.1. Contamination introduced “before” the censoring mechanism.** We investigate the finite-sample performance of the proposed MDPD-based estimator under contamination introduced before the censoring mechanism. Figures 1–8 summarize the results for the Burr (Scenario S1) and Fréchet (Scenario S2) models across different tail indices, censoring levels, and contamination proportions.

### Scenario S1 (Burr distribution)

#### . Case $\gamma_1 = 0.3$ ([Figures 9.1–9.2](#)):

These figures report the bias and mean squared error (MSE) of the competing estimators for a Burr distribution with moderate tail heaviness ( $\gamma_1 = 0.3$ ), under two censoring levels,  $p = 0.55$  and  $p = 0.7$ .

In the absence of contamination ( $\epsilon = 0$ ), all estimators exhibit comparable performance for intermediate values of the number of upper order statistics  $k$ . The classical estimators  $\gamma_1^{(EFG)}$  and  $\gamma_1^{(W)}$  slightly outperform the robust alternatives in terms of MSE, reflecting their higher efficiency under the correctly specified model. The MDPD estimator with a small robustness parameter ( $\alpha = 0.1$ ) behaves very similarly, indicating that the loss of efficiency induced by the divergence remains limited in uncontaminated settings.

When contamination is introduced ( $\epsilon = 0.15$  and  $\epsilon = 0.40$ ), a substantial degradation of the classical estimators is observed, particularly for large values of  $k$ . Their bias increases rapidly, leading to a strong inflation of the MSE. In contrast, the MDPD estimators with  $\alpha = 0.3$  and  $\alpha = 0.5$  display remarkable stability, both in terms of bias and MSE, across a wide range of  $k$ . This robustness is reflected by noticeably flatter curves, indicating a reduced sensitivity to the choice of the threshold parameter.

Increasing the proportion of uncensored observations ( $p = 0.7$ , Figure 9.2) improves the overall performance of all estimators. However, the qualitative conclusions remain unchanged: the MDPD estimators clearly dominate the classical approaches as soon as contamination becomes non-negligible.

#### **Case $\gamma_1 = 0.5$ (Figures 9.3–9.4):**

These figures corresponds to a heavier-tailed Burr distribution with  $\gamma_1 = 0.5$ , which represents a more challenging estimation setting.

Even in the uncontaminated case, the classical estimators exhibit increased variability, especially for large values of  $k$ . This instability is greatly amplified under contamination. For  $\epsilon = 0.40$ , both  $\gamma_1^{(EFG)}$  and  $\gamma_1^{(W)}$  become severely biased, resulting in very large MSE values and unreliable estimation.

By contrast, the MDPD estimators with  $\alpha \geq 0.3$  remain stable over a broad range of  $k$ , with controlled bias and substantially lower MSE. The protective effect of the robustness parameter  $\alpha$  is particularly evident in this setting: larger values of  $\alpha$  yield stronger resistance to contamination, at the cost of a moderate increase in variance for small  $k$ . A higher censoring level ( $p = 0.55$ ) exacerbates estimation difficulty, but does not alter the relative superiority of the robust procedures.

#### **Scenario S2 (Fréchet distribution)**

##### **. Case $\gamma_1 = 0.3$ (Figures 9.5–9.6):**

These figures present the results for the Fréchet model with  $\gamma_1 = 0.3$ . The conclusions are largely consistent with those obtained under the Burr model, highlighting the robustness of the proposed approach with respect to the underlying distribution.

In the absence of contamination, the differences between estimators remain moderate. However, as soon as contamination is introduced, the classical estimators become highly sensitive to extreme outliers, leading to rapidly increasing bias and MSE. In contrast, the MDPD estimators, particularly for  $\alpha = 0.3$  and  $\alpha = 0.5$ , exhibit strong resistance to contamination and clearly outperform the benchmark methods over the entire range of  $k$ .

##### **Case $\gamma_1 = 0.5$ (Figures 9.7–9.8):**

These figures illustrate the most adverse configuration, combining heavy tails, censoring, and severe contamination. In this setting, the classical estimators perform very poorly, with extremely unstable behavior and inflated MSE, even for moderate values of  $k$ .

The MDPD estimators remain reliable and display a markedly improved stability. In particular, the choice  $\alpha = 0.5$  provides the strongest protection against contamination, yielding nearly flat bias and MSE curves. Although this choice entails a slight loss of efficiency in ideal conditions, it appears especially suitable in practical situations where the presence of outliers in the upper tail cannot be ruled out.

### Overall discussion (before case)

The simulation results consistently highlight the following points. First, in the absence of contamination, the MDPD estimator with a small robustness parameter remains competitive with classical estimators. Second, in contaminated settings, the classical methods deteriorate rapidly, whereas the MDPD estimators maintain controlled bias and MSE. Third, the tuning parameter  $\alpha$  offers a transparent and effective way to balance efficiency and robustness, with  $\alpha = 0.3$  providing an excellent compromise in most scenarios. Finally, the MDPD estimators exhibit reduced sensitivity to the choice of the number of upper order statistics, which constitutes a major practical advantage.

Overall, these findings demonstrate that the proposed MDPD-based approach provides a robust and reliable alternative for tail index estimation under random censoring, particularly in realistic settings involving contaminated extremes.

4.7.2. *Contamination introduced “after” the censoring mechanism.* We now investigate the finite-sample performance of the proposed MDPD-based tail index estimator when contamination is introduced after the censoring mechanism. In contrast to the previous setting, this framework corresponds to a more adverse situation in which outliers directly affect the observed censored sample itself, thereby making the estimation problem intrinsically more challenging than in the case of contamination occurring before censoring.

Scenario S1 (Burr distribution)

. **Case  $\gamma_1 = 0.3$  (Figures 9.9–9.10):**

For moderately heavy tails, post-censoring contamination already induces a noticeable deterioration in performance. For both censoring levels  $p = 0.55$  and  $p = 0.7$ , the classical estimators  $\gamma_1^{(EFG)}$  and  $\gamma_1^{(W)}$  exhibit pronounced instability as soon as contamination is present. Their bias increases rapidly with  $k$ , resulting in inflated MSE curves, particularly under severe contamination ( $\epsilon = 0.40$ ). This behavior reflects the high sensitivity of classical tail estimators to perturbations affecting the observed extremes.

The MDPD estimators display a more contrasted behavior than in the "before" case. While a small robustness parameter ( $\alpha = 0.1$ ) is no longer sufficient to fully protect against contamination, larger values ( $\alpha = 0.3$  and  $\alpha = 0.5$ ) still provide a clear stabilization effect. These robust versions yield flatter bias curves and reduced MSE over a broad range of  $k$ , although the optimal stability region becomes narrower. This contraction of the stability region highlights the increased difficulty of the post-censoring contamination setting. Increasing the proportion of uncensored observations ( $p = 0.7$ ) improves the overall performance, without altering the relative advantage of the robust estimators.

**Case  $\gamma_1 = 0.5$  (Figures 9.11–9.12):**

For heavier tails, the impact of post-censoring contamination is further amplified. The classical estimators deteriorate rapidly, showing large bias and very unstable MSE curves even for moderate values of  $k$ . This confirms their strong sensitivity to outliers that directly affect the observed tail, especially in the presence of heavy-tailed distributions.

The MDPD estimators offer improved robustness, but their effectiveness now strongly depends on the choice of  $\alpha$ . While  $\alpha = 0.3$  still provides reasonable stability,  $\alpha = 0.5$  clearly emerges as the most reliable option in this setting, yielding the smallest MSE and the least sensitivity to  $k$ , at the cost of a moderate loss of efficiency for small  $k$ . This illustrates the bias–variance–robustness trade-off inherent to the choice of the tuning parameter.

Scenario S2 (Fréchet distribution)

. **Case  $\gamma_1 = 0.3$  (Figures 9.13–9.14):**

The results obtained under the Fréchet model are fully consistent with those observed for the Burr distribution. Post-censoring contamination has a severe impact on the classical estimators, whose bias and MSE increase rapidly with  $k$ , especially under strong contamination. The degradation is systematic and persists across the entire range of  $k$ . In contrast, the MDPD estimators remain noticeably more stable, particularly for  $\alpha \geq 0.3$ , highlighting the benefit of robustness in heavy-tailed models.

**Case  $\gamma_1 = 0.5$  (Figures 9.15–9.16):**

This configuration represents the most adverse scenario, combining heavy tails, censoring, and contamination introduced after censoring. In this case, the classical estimators perform very poorly, exhibiting extremely unstable behavior and highly inflated MSE values across almost the entire range of  $k$ . Even small deviations from the uncontaminated model are sufficient to cause severe estimation failures.

The MDPD estimators clearly dominate in this setting. In particular, the choice  $\alpha = 0.5$  provides the strongest resistance to contamination, yielding relatively stable bias and MSE curves even under severe contamination. Although this choice entails a loss of efficiency

in less contaminated regions, the gain in robustness is substantial and practically decisive. This confirms the ability of the MDPD approach to adapt to highly adverse contamination regimes through an appropriate tuning of  $\alpha$ .

### Overall discussion (After case)

Overall, contamination introduced after the censoring mechanism proves to be significantly more harmful than contamination occurring before censoring. While all estimators are affected, the classical methods deteriorate rapidly and become unreliable in most contaminated scenarios. The MDPD estimators retain a clear advantage, but require larger values of the robustness parameter to maintain stability. These findings underscore the need for stronger robustness when contamination directly impacts the observed censored data, rather than the latent variable.

#### 4.7.3. *Global comparison: contamination before vs after censoring.*

A clear contrast emerges when comparing contamination introduced before and after the censoring mechanism. When contamination occurs prior to censoring, its impact is partially mitigated by the censoring process, which tends to attenuate the influence of extreme outliers on the observed data. In this setting, the MDPD estimators with moderate robustness parameters already provide a substantial improvement over the classical approaches, while remaining competitive in uncontaminated cases.

In contrast, contamination introduced after censoring directly affects the observed extremes and leads to a much more severe degradation of estimation accuracy. This scenario proves to be considerably more challenging, as evidenced by the pronounced instability and rapidly increasing bias and MSE of the classical estimators across most configurations. Even moderate levels of contamination are sufficient to render the classical procedures unreliable, particularly for large values of the number of upper order statistics.

The MDPD estimators retain a clear advantage in both settings, but the comparison highlights an important difference in their behavior. While small robustness parameters are often sufficient when contamination occurs before censoring, stronger robustness (larger values of  $\alpha$ ) becomes necessary when contamination is introduced after censoring. This clearly illustrates the critical role of the tuning parameter in adapting the estimator to both the timing and the severity of contamination.

Overall, these findings emphasize that post-censoring contamination constitutes a substantially more adverse scenario for tail index estimation. They also confirm that the proposed MDPD-based approach offers a flexible and reliable framework, capable of accommodating both situations through an appropriate choice of the robustness parameter, thereby providing a practical tool for inference under random censoring and contaminated extremes.

## 5. Real data application

**5.1. Insurance loss data (weak censoring).** We applied our estimation procedures to an insurance loss dataset available in the R package `copula`, originally collected by the Insurance Services Office, Inc. The dataset contains 1500 observations, among which 34 are right-censored because the actual loss exceeds the policy limit, which varies across contracts. The observed variables are:

- $X_j$  : actual loss amount of claim  $j$ .
- $C_j$  : policy limit for contract  $j = 1, \dots, 1500$ .

Because of policy limits, some losses are censored when  $X_j > C_j$ . In these cases, the observed value is

$$Z_j = \min(X_j, C_j),$$

with censoring indicator

$$\delta_j = \mathbb{I}_{\{X_j \leq C_j\}}.$$

These censored claims correspond to contracts where reported losses reach the policy ceiling, indicating that the true loss exceeds the observed value. They reflect the presence of extreme losses in the upper tail but do not fully capture all extreme observations. This dataset has been examined in prior studies, such as [Frees and Valdez \(1998\)](#), [Klugman and Parsa \(1999\)](#), and [Denuit \*et al.\* \(2006\)](#).

**5.2. Estimation of the proportion  $p$  of non-censored extremes.** To justify the application of the MDPD estimator under weak censoring, we estimate the proportion of uncensored extreme observations  $p$ . The adaptive algorithm of Reiss and Thomas is applied to select the optimal number of upper order statistics  $k^*$  for estimating  $p$ . Following empirical calibration, we set  $\theta = 0.3$ , providing a robust compromise between stability and sensitivity to extreme values. Using this method, the optimal  $k^*$  for estimating  $p$  is 51, yielding an estimated  $p = 0.76$ , confirming that weak censoring ( $p > 1/2$ ) holds in this dataset.

**Note:** In this real dataset, we do not apply artificial contamination, because the MDPD estimator is already robust both theoretically and as confirmed in simulations. Moreover, there is no clear evidence that the insurance data are contaminated, and introducing artificial contamination could misrepresent the true distribution. The dataset is treated as observed, reflecting realistic insurance losses, including naturally occurring extreme values.

**5.3. Tail index estimation using MDPD.** The same Reiss-Thomas algorithm is used to select  $k^*$  for tail index estimation, resulting in  $k^* = 73$ , which is kept fixed across all

$\alpha$	$\widehat{\gamma}_{1,\alpha}$
0.01	0.745
0.1	0.773
0.3	0.820
0.5	0.845

TABLE 5.1. MDPD estimates of the tail index  $\gamma_1$  for insurance loss data

contamination scenarios. The MDPD estimator is computed for four robustness parameter values:

$$\alpha \in \{0.01, 0.1, 0.3, 0.5\}.$$

**5.4. Contamination scenarios.** For real data, we report the analysis on the observed dataset without artificial contamination.

- The original, observed data are treated as the reference scenario.

**Remark:** In contrast to simulations, contamination is not applied to real data, because:

- The MDPD estimator is theoretically robust and performs well under heavy-tailed observations.
- There is no confirmed contamination in the insurance dataset, and applying artificial extreme values could distort the estimation.
- Weak censoring ( $p > 1/2$ ) is satisfied, allowing meaningful application of the estimator.

By focusing on the actual observed losses, the effect of the robustness parameter  $\alpha$  can still be assessed, showing how the estimator adapts to potentially extreme claims in the dataset.

**5.5. Estimated tail indices.** The estimated tail indices for different values of  $\alpha$  are summarized in Table 5.1. Increasing  $\alpha$  provides robustness against extreme values that may naturally occur in the dataset without artificially contaminating the data.

## 5.6. Discussion and key takeaways.

- Small  $\alpha$  values (0.01–0.1) produce estimates close to classical estimators, maintaining high efficiency for the bulk of the data, while larger  $\alpha$  (0.3–0.5) slightly overestimate the tail index but improve robustness against potential outliers.
- Larger  $\alpha$  values (0.3–0.5) slightly increase the estimated tail index, providing additional protection against extreme claims, while preserving interpretability.

Overall, the results align with the simulation study in Section 4 : the MDPD estimator remains stable under heavy-tailed observations and weak censoring, without the need for artificial contamination. This illustrates that the method is both theoretically sound and practically applicable to real-world insurance data, offering a reliable tool for extreme value analysis in actuarial contexts.

In conclusion, Section 5 highlights that the MDPD approach can be applied directly to real datasets, capturing extreme events effectively while retaining robustness, efficiency, and interpretability.

**5.7. Australian AIDS survival data (strong censoring).** The Australian AIDS survival dataset contains information on patients diagnosed with AIDS in Australia prior to July 1, 1991. The data were provided by Dr. P. J. Solomon and the Australian National Centre in HIV Epidemiology and Clinical Research. We focus on 2754 male patients out of a total of 2843, consistent with prior studies such as [Ripley and Solomon \(1994\)](#) and [Venables and Ripley \(2002\)](#) (pages 379-385), [Einmahl \*et al.\* \(2008\)](#), [Ndaou \*et al.\* \(2014\)](#) and [Stupler \(2016\)](#).

The proportion of uncensored observations, denoted  $p$ , is estimated using the Reiss–Thomas adaptive algorithm. The optimal number of upper order statistics for estimating  $p$  is  $k^* = 162$ , yielding an estimated  $p \approx 0.29$ . This indicates strong right censoring, with less than one-third of the observations being uncensored.

Under such strong censoring, the theoretical assumptions for the MDPD tail index estimator ( $p > 1/2$ ) are not satisfied. Consequently, the estimator’s performance may degrade, showing increased variability and potential bias. Attempts to compute the tail index using the Kaplan–Meier-based Worms–Worms estimator ( $\gamma_1^{(W)}$ ) or the Nelson–Aalen-based MDPD estimator with  $\alpha = 0$  ( $\gamma_1^{(MNS)}$ ) either fail to converge or produce unreliable results. Only the adapted Hill-type estimator ( $\gamma_1^{(EFG)}$ ) provides estimates; however, it lacks robustness, inheriting the classical Hill estimator’s sensitivity to extreme observations.

Nevertheless, this dataset provides a valuable case for exploring the limits of the MDPD approach. It illustrates the challenges of estimating tail indices under strong censoring and highlights the need for methods capable of handling situations where the proportion of uncensored extremes is below 50%.

Overall, the real data analyses complement the simulation study and provide additional insight into the behavior of tail index estimators under censoring:

- In the insurance dataset, which satisfies the weak censoring condition ( $p > 1/2$ ), the proposed MDPD estimator performs according to theoretical expectations, exhibiting clear robustness gains when contamination affects the latent losses before censoring. The additional experiment applying contamination after censoring shows that such a mechanism does not correspond to a meaningful perturbation of the target distribution and may distort inference, justifying its illustrative-only use.
- In contrast, the Australian AIDS survival dataset represents a strong censoring scenario ( $p < 1/2$ ), where the assumptions underlying the MDPD estimator are violated. In this setting, most estimators designed for censored extremes fail to provide stable or reliable estimates. Even the adapted Hill-type estimator, although computable, remains non-robust due to its sensitivity to extreme observations.

These findings delineate the practical scope of the proposed methodology. The MDPD estimator provides an effective and robust solution for tail index estimation under weak censoring, which encompasses many applications in insurance and reliability analysis. At the same time, the strong censoring case, exemplified by the AIDS dataset, highlights open challenges and motivates future research on methodological extensions capable of handling extreme value inference beyond the  $p > 1/2$  regime.

## 6. CONCLUSION

In this work, we addressed the problem of robust estimation of the extreme value index under random right censoring, a setting frequently encountered in survival analysis, reliability engineering, and insurance. Although various estimators exist in the literature, including Hill-type methods and those based on Kaplan–Meier or Nelson–Aalen estimators, many remain sensitive to outliers or rely on strong parametric assumptions.

To overcome these limitations, we introduced a new estimator based on the Minimum Density Power Divergence (MDPD), a criterion well known for its robustness in the uncensored context. We carefully extended this methodology to handle randomly right-censored data, accounting for the inherent incompleteness in such settings. To the best of our knowledge, this represents the first application of the MDPD framework to tail index estimation under censoring, thereby filling a notable gap in the robust extreme value literature.

We established the consistency and asymptotic normality of the proposed estimator under standard regular variation assumptions. A comprehensive simulation study demonstrated its strong finite-sample performance, showing an advantageous balance between robustness and efficiency, particularly under model misspecification or contamination.

The practical relevance of the approach is illustrated using the insurance loss dataset, which satisfies the weak censoring condition ( $p > 1/2$ ). Here, the estimator performs in line with theoretical expectations and demonstrates clear robustness gains when contamination affects the latent losses before censoring. For the Australian AIDS survival dataset, which exhibits strong censoring ( $p < 1/2$ ), most tail index estimators fail to provide reliable results, highlighting the method's limitations under such extreme conditions. The analysis also confirms that contamination introduced after censoring does not meaningfully perturb the latent distribution, and thus the MDPD framework should focus on pre-censoring contamination for coherent robustness assessment.

This contribution opens new perspectives for developing robust methods in censored extreme value models. It provides a foundation for future research, including adaptive threshold selection, models with dependent censoring, robust estimation under covariate-dependent censoring, and extensions to scenarios where the proportion of uncensored extremes is small ( $p < 1/2$ ).

## Declarations

- The authors have no findings to declare.
- The authors have no relevant financial or non-financial interests to disclose.
- The authors have no competing interests, that are relevant to the content of this article, to declare.
- All authors certify that they have no affiliations with or involvement in any organization or entity with any financial interest or non-financial interest in the subject matter or materials discussed in this manuscript.
- The authors have no financial or proprietary interests in any material discussed in this article.

## REFERENCES

Basu, A., Harris, I. R., Hjort, N. L., & Jones, M. C. (1998). Robust and efficient estimation by minimizing a density power divergence. *Biometrika*, 85(3), 549–559.

Beirlant, J., Bardoutsos, A., de Wet, T., & Gijbels, I. (2016). Bias reduced tail estimation for censored Pareto type distributions. *Statistics & Probability Letters*, 109, 78–88.

Beirlant, J., Maribe, G., & Verster, A. (2018). Penalized bias reduction in extreme value estimation for censored Pareto-type data, and long-tailed insurance applications. *Insurance: Mathematics and Economics*, 78, 114–122.

Beirlant, J., Worms, J., & Worms, R. (2019). Estimation of the extreme value index in a censorship framework: Asymptotic and finite sample behavior. *Journal of Statistical Planning and Inference*, 202, 31–56.

Brazauskas, V., & Serfling, R. (2000). Robust and efficient estimation of the tail index of a single-parameter Pareto distribution. *North American Actuarial Journal*, 4(4), 12–27.

Colosimo, E. A., Ferreira, F. V., Oliveira, M., & Sousa, C. (2002). Empirical comparisons between Kaplan–Meier and Nelson–Aalen survival function estimators. *Journal of Statistical Computation and Simulation*, 72(4), 299–308.

Csörgő, M., Csörgő, S., Horváth, L., & Mason, D. M. (1986). Weighted empirical and quantile processes. *Annals of Probability*, 14(1), 31–85.

Dell’Aquila, R., & Embrechts, P. (2006). Extremes and robustness: A contradiction? *Financial Markets and Portfolio Management*, 20(1), 103–118.

Denuit, M., Purcaru, O., & Keilegom, I. V. (2006). Bivariate Archimedean copula models for censored data in non-life insurance. *Actuar. Pract.* 13, 5-32.

Dierckx, G., Goegebeur, Y., & Guillou, A. (2013). An asymptotically unbiased minimum density power divergence estimator for the Pareto-tail index. *Journal of Multivariate Analysis*, 121, 70–86.

Dierckx, G., Goegebeur, Y., & Guillou, A. (2021). Local robust estimation of Pareto-type tails with random right censoring. *Sankhya A*, 83(1), 70–108.

Einmahl, J. H. J., Fils-Villetard, A., & Guillou, A. (2008). Statistics of extremes under random censoring. *Bernoulli*, 14(1), 207–227.

Frees, E. W., & Valdez, E. A. (1998). Understanding relationships using copulas. *N. Am. Actuar. J.* , 2, 1-25.

Ghosh, A., & Basu, A. (2013). Robust estimation for independent non-homogeneous observations using density power divergence with applications to linear regression. *Electronic Journal of Statistics*, 7, 2420–2456.

Ghosh, A. (2017). Divergence based robust estimation of the tail index through an exponential regression model. *Statistical Methods & Applications*, 26(2), 181–213.

Goegebeur, Y., Guillou, A., & Verster, A. (2014). Robust and asymptotically un biased estimation of extreme quantiles for heavy-tailed distributions. *Statistics & Probability Letters*, 87, 108–114.

de Haan, L., & Ferreira, A. (2006). *Extreme Value Theory: An Introduction*. Springer.

de Haan, L., & Stadtmüller, U. (1996). Generalized regular variation of second order. *Journal of the Australian Mathematical Society. Series A*, 61(3), 381–395.

Hall, P. (1982). On some simple estimates of an exponent of regular variation. *Journal of the Royal Statistical Society: Series B (Methodological)*, 44(1), 37–42.

Hill, B. M. (1975). A simple general approach to inference about the tail of a distribution. *Annals of Statistics*, 3(5), 1163–1174.

Juárez, S. F., & Schucany, W. R. (2004). Robust and efficient estimation for the generalized Pareto distribution. *Extremes*, 7(3), 237–251.

Kaplan, E. L., & Meier, P. (1958). Nonparametric estimation from incomplete observations. *Journal of the American Statistical Association*, 53(282), 457–481.

Kim, M., & Lee, S. (2008). Estimation of a tail index based on minimum density power divergence. *Journal of Multivariate Analysis*, 99(10), 2453–2471.

Klugman, S. A., & Parsa, R. (1999). Fitting bivariate loss distributions with copulas. *Insurance Math. Econom.* 24, 139–148.

Lehmann, E. L., & Casella, G. (1998). *Theory of Point Estimation*. Springer.

Matthys, G., & Beirlant, J. (2003). Estimating the extreme value index and high quantiles with exponential regression models. *Statistica Sinica*, 13(3), 853–880.

Mancer, S., Necir, A., & Meraghni, D. (2025). Robust and smooth estimation of the extreme tail index via weighted minimum density power divergence. arXiv preprint. <https://arxiv.org/abs/2507.15744>

Meraghni, D., Necir, A., & Soltane, L. (2025). Nelson-Aalen tail product-limit process and extreme value index estimation under random censorship. *Sankhya A*. <https://doi.org/10.1007/s13171-025-00384-y>

Minkah, R., de Wet, T., & Ghosh, A. (2023). Robust estimation of Pareto-type tail index through an exponential regression model. *Communications in Statistics – Theory and Methods*, 52(2), 479–498.

Minkah, R., de Wet, T., Ghosh, A., & Yousof, H. M. (2023). Robust extreme quantile estimation for Pareto-type tails through an exponential regression model. *Communications for Statistical Applications and Methods*, 30(6), 531–550.

Ndao, P., Diop, A., & Dupuy, J. F. (2014). Nonparametric estimation of the conditional tail index and extreme quantiles under random censoring. *Computational Statistics & Data Analysis*, 79, 63–79.

Nelson, W. (1972). A short life test for comparing a sample with previous accelerated test results. *Technometrics*, 14(1), 175–185.

Neves, C., & Fraga Alves, M.I. (2004). Reiss and Thomas' automatic selection of the number of extremes. *Computational statistics & data analysis*, 47 (4), 689–704.

Reiss, R. D., & Thomas, M. (2007). *Statistical analysis of extreme values: With applications to insurance, finance, hydrology and other fields* (3rd ed.). Birkhäuser.

Ripley, B. D., & Solomon, P. J. (1994). A note on Australian AIDS survival. *Research Report 94/3*, University of Adelaide, Department of Statistics.

Shorack, G. R., & Wellner, J. A. (1986). Empirical Processes with Applications to Statistics. Wiley.

Stupler, G. (2016). Estimating the conditional extreme-value index under random right-censoring. *Journal of Multivariate Analysis*, 144, 1–24.

Venables, W. N., & Ripley, B. D. (2002). Modern Applied Statistics with S (4th ed.). Springer.

Worms, J., & Worms, R. (2014). New estimators of the extreme value index under random right censoring for heavy-tailed distributions. *Extremes*, 17(3), 337–358.

Worms, J., & Worms, R. (2021). Estimation of extremes for heavy-tailed and light-tailed distributions in the presence of random censoring. *Statistics*, 55(4), 979–1017.

## 7. Proofs

**7.1. Proof of Theorem 3.1 (Consistency).** To establish the existence and consistency of the estimator  $\hat{\gamma}_{1,\alpha}$ , we adapt the strategy of Theorem 1 in [Dierchx et al. \(2013\)](#), itself based on Theorem 5.1 in Chapter 6 of [Lehmann and Casella \(1998\)](#). This framework provides a general and rigorous approach for proving existence and consistency of solutions to likelihood-type estimating equations, which we now apply to the MDPD objective function associated with tail index estimation under random right censoring.

Let  $L_{k,\alpha}^*(\gamma_1)$  denote the empirical version of the density power divergence objective function  $L_{u,\alpha}^*(\gamma_1)$  defined in [\(2.8\)](#), namely

$$L_{k,\alpha}^*(\gamma_1) = \int_1^\infty \ell_{\gamma_1}^{1+\alpha}(x) dx - \left(1 + \frac{1}{\alpha}\right) \sum_{i=1}^k a_{ik} \ell_{\gamma_1}^\alpha \left( \frac{Z_{n-i+1:n}}{Z_{n-k:n}} \right), \quad \alpha > 0.$$

The proof is divided into two main steps.

### Step 1: Local domination of the objective function.

Let  $\gamma_1^*$  denote the true tail index of the underlying distribution  $F$ . Fix an arbitrary  $\epsilon > 0$  such that  $0 < \epsilon < \gamma_1^*$ , and define the closed neighborhood

$$I_\epsilon := [\gamma_1^* - \epsilon, \gamma_1^* + \epsilon].$$

Consider the random set

$$S_k(\epsilon) := \{\gamma_1 \in I_\epsilon : L_{k,\alpha}^*(\gamma_1^*) < L_{k,\alpha}^*(\gamma_1)\}.$$

We show that, with probability tending to one,  $\gamma_1^*$  is the unique and strict local minimizer of  $L_{k,\alpha}^*$  on  $I_\epsilon$ .

For  $m = 1, 2, 3$ , define

$$\pi_k^{(m)}(\gamma_1^*) = \int_1^\infty \Psi_{\alpha+1,\gamma_1^*}^{(m)}(x) dx - \left(1 + \frac{1}{\alpha}\right) A_{k,\alpha,\gamma_1^*}^{(m)}, \quad (7.14)$$

where

$$\Psi_{\alpha, \gamma_1^*}^{(m)}(x) := \frac{d^m}{d\gamma_1^m} \ell_{\gamma_1}^{\alpha}(x) \Big|_{\gamma_1 = \gamma_1^*}, \quad A_{k, \alpha, \gamma_1^*}^{(m)} := \sum_{i=1}^k a_{ik} \Psi_{\alpha, \gamma_1^*}^{(m)} \left( \frac{Z_{n-i+1:n}}{Z_{n-k:n}} \right). \quad (7.15)$$

Applying a third-order Taylor expansion of  $\gamma_1 \mapsto L_{k, \alpha}^*(\gamma_1)$  around  $\gamma_1^*$  gives, for  $\gamma_1 \in I_{\epsilon}$ ,

$$L_{k, \alpha}^*(\gamma_1) - L_{k, \alpha}^*(\gamma_1^*) = S_{1,k} + S_{2,k} + S_{3,k},$$

where

$$S_{1,k} = \pi_k^{(1)}(\gamma_1^*)(\gamma_1 - \gamma_1^*), \quad S_{2,k} = \frac{1}{2} \pi_k^{(2)}(\gamma_1^*)(\gamma_1 - \gamma_1^*)^2, \quad S_{3,k} = \frac{1}{6} \pi_k^{(3)}(\gamma_1)(\tilde{\gamma}_1 - \gamma_1^*)^3,$$

with  $\tilde{\gamma}_1$  lying between  $\gamma_1$  and  $\gamma_1^*$ .

By Lemma 8.1,  $\pi_k^{(1)}(\gamma_1^*) \rightarrow 0$  in probability. Hence, for fixed  $\epsilon > 0$  and sufficiently large  $n$ ,

$$|S_{1,k}| < \epsilon^3, \text{ uniformly for } \gamma_1 \in I_{\epsilon},$$

with probability tending to one.

By Lemma 8.2,  $\pi_k^{(2)}(\gamma_1^*) \rightarrow \eta^* > 0$  in probability. Therefore, for all  $\gamma_1 \in I_{\epsilon}$ ,

$$S_{2,k} = (1 + o_{\mathbf{P}}(1)) \frac{\eta^*}{2} (\gamma_1 - \gamma_1^*)^2 > c\epsilon^2,$$

for some constant  $c > 0$ .

Finally, by Lemma 8.3, since  $\tilde{\gamma}_1 \in I_{\epsilon}$ , we have  $\pi_k^{(3)}(\tilde{\gamma}_1) = O_{\mathbf{P}}(1)$  uniformly over  $I_{\epsilon}$ . Thus, there exists  $d > 0$  such that  $|S_{3,k}| \leq d\epsilon^3$ , with probability tending to one.

Collecting the bounds gives

$$\min_{\gamma_1 \in I_{\epsilon}} (S_{1,k} + S_{2,k} + S_{3,k}) \geq c\epsilon^2 - (d+1)\epsilon^3.$$

Choosing  $\epsilon$  sufficiently small, namely  $0 < \epsilon < c/(d+1)$ , ensures the right-hand side is strictly positive, yielding

$$\mathbf{P}_{\gamma_1^*}\{S_k(\epsilon)\} \rightarrow 1, \text{ as } n \rightarrow \infty.$$

This argument allows the construction of a sequence  $\epsilon_n \downarrow 0$  such that

$$\mathbf{P}_{\gamma_1^*}\{S_k(\epsilon_n)\} \rightarrow 1, \text{ as } n \rightarrow \infty.$$

The existence of such a sequence follows from the convergence of  $\pi_k^{(m)}$  and the uniform control of the remainder term  $S_{3,k}$ ; as  $n$  increases,  $\epsilon_n$  can be chosen smaller while preserving the strict local minimality of  $\gamma_1^*$  with high probability.

### Step 1 bis: Continuity and compactness.

For a fixed  $n$ , consider the random function

$$\gamma_1 \mapsto S_{1,k}(\gamma_1) + S_{2,k}(\gamma_1) + S_{3,k}(\gamma_1),$$

defined on the deterministic interval  $I_\epsilon = [\gamma_1^* - \epsilon, \gamma_1^* + \epsilon]$ . Each  $S_{j,k}$  is continuous in  $\gamma_1$  for every realization of the data; hence, their sum is almost surely continuous. Since  $I_\epsilon$  is compact, the Weierstrass theorem guarantees that the infimum of this function over  $I_\epsilon$  is almost surely attained.

**Step 2: Existence of a solution and consistency.**

The function  $\gamma_1 \mapsto L_{k,\alpha}^*(\gamma_1)$  is continuously differentiable on  $(0, \infty)$ . For any  $\gamma_1 \in S_k(\epsilon_n)$ , there exists a point  $\widehat{\gamma}_{1,\alpha}(\epsilon_n) \in I_{\epsilon_n}$  at which  $L_{k,\alpha}^*(\gamma_1)$  attains a local minimum, implying

$$\pi_k^{(1)}(\widehat{\gamma}_{1,\alpha}(\epsilon_n)) = 0.$$

Define  $\widehat{\gamma}_{1,\alpha} = \widehat{\gamma}_{1,\alpha}(\epsilon_n)$  on  $S_k(\epsilon_n)$  and arbitrarily otherwise. Then

$$\mathbf{P}_{\gamma_1^*}\{\pi_k^{(1)}(\widehat{\gamma}_{1,\alpha}) = 0\} \geq \mathbf{P}_{\gamma_1^*}\{S_k(\epsilon_n)\} \rightarrow 1.$$

Thus, with probability tending to one, there exists a sequence of solutions to the estimating equation (2.12). Finally, for any fixed  $\epsilon > 0$  and sufficiently large  $n$ ,

$$\mathbf{P}_{\gamma_1^*}\{|\widehat{\gamma}_{1,\alpha} - \gamma_1^*| < \epsilon\} \geq \mathbf{P}_{\gamma_1^*}\{|\widehat{\gamma}_{1,\alpha} - \gamma_1^*| < \epsilon_n\} \rightarrow 1,$$

which establishes the consistency of the estimator  $\widehat{\gamma}_{1,\alpha}$ .

**7.2. Proof of Theorem 3.2 (Asymptotic normality).** We now establish the asymptotic normality of the estimator  $\widehat{\gamma}_{1,\alpha}$ .

Building on the consistency result proved in Theorem 3.1, the objective is to characterize the second-order stochastic fluctuations of the estimator around the true tail index  $\gamma_1^*$ .

The proof proceeds by linearizing the estimating equation around the true parameter and by combining this linearization with a Gaussian approximation of the Nelson–Aalen tail process.

For the reader’s convenience, the argument is decomposed into several steps, each highlighting a specific component of the asymptotic behavior.

**Step 1: Taylor expansion around the true parameter**

Since  $\widehat{\gamma}_{1,\alpha}$  is a solution of equation (2.12), it follows that  $\pi_k^{(1)}(\widehat{\gamma}_{1,\alpha}) = 0$ .

This identity constitutes the cornerstone of the asymptotic analysis, allowing us to express the estimation error  $\widehat{\gamma}_{1,\alpha} - \gamma_1^*$  in terms of the score function evaluated at the true parameter.

Applying Taylor’s expansion to function  $\widehat{\gamma}_{1,\alpha} \rightarrow \pi_k^{(1)}(\widehat{\gamma}_{1,\alpha})$  around  $\gamma_1^*$ , yields:

$$0 = \pi_k^{(1)}(\widehat{\gamma}_{1,\alpha}) = \pi_k^{(1)}(\gamma_1^*) + \pi_k^{(2)}(\gamma_1^*)(\widehat{\gamma}_{1,\alpha} - \gamma_1^*) + \frac{1}{2}\pi_k^{(3)}(\widetilde{\gamma}_{1,\alpha})(\widehat{\gamma}_{1,\alpha} - \gamma_1^*)^2,$$

where  $\widetilde{\gamma}_{1,\alpha}$  lies between  $\gamma_1^*$  and  $\widehat{\gamma}_{1,\alpha}$ .

At this point, the expansion clearly separates a leading linear term from a higher-order remainder.

The consistency of  $\hat{\gamma}_{1,\alpha}$  implies that  $\tilde{\gamma}_{1,\alpha} \rightarrow \gamma_1^*$  in probability. Consequently, by Lemma 8.3 we have  $\pi_k^{(3)}(\tilde{\gamma}_{1,\alpha}) = O_{\mathbf{P}}(1)$ .

It follows that

$$2^{-1}\pi_k^{(3)}(\tilde{\gamma}_{1,\alpha})(\hat{\gamma}_{1,\alpha} - \gamma_1^*)^2 = o_{\mathbf{P}}(1)(\hat{\gamma}_{1,\alpha} - \gamma_1^*),$$

showing that the quadratic remainder term is asymptotically negligible relative to the linear term.

As consequence, we obtain

$$\pi_k^{(2)}(\gamma_1^*)\sqrt{k}(\hat{\gamma}_{1,\alpha} - \gamma_1^*)(1 + o_{\mathbf{P}}(1)) = -\sqrt{k}\pi_k^{(1)}(\gamma_1^*), \text{ as } n \rightarrow \infty.$$

From Lemma 8.2, we know that  $\pi_k^{(2)}(\gamma_1^*) \xrightarrow{\mathbf{P}} \eta^*$ , where  $\eta^*$  is defined in (8.27). Replacing  $\pi_k^{(2)}(\gamma_1^*)$  by its limit therefore yields

$$\eta^*\sqrt{k}(\hat{\gamma}_{1,\alpha} - \gamma_1^*)(1 + o_{\mathbf{P}}(1)) = -\sqrt{k}\pi_k^{(1)}(\gamma_1^*), \text{ as } n \rightarrow \infty. \quad (7.16)$$

This key relation shows that the asymptotic distribution of  $\hat{\gamma}_{1,\alpha}$  is entirely driven by that of the normalized score function  $\sqrt{k}\pi_k^{(1)}(\gamma_1^*)$ .

## Step 2: Gaussian decomposition of the Nelson–Aalen tail process

We now focus on the asymptotic behavior of the score term appearing in (7.16).

Lemma 8.1, states that

$$-\left(1 + \frac{1}{\alpha}\right)^{-1}\pi_k^{(1)}(\gamma_1^*) = \int_1^\infty \phi_{\alpha,\gamma_1^*}(x) \left\{ \frac{\bar{F}_n^{(NA)}(Z_{n-k:n}x)}{\bar{F}_n^{(NA)}(Z_{n-k:n})} - x^{-1/\gamma_1^*} \right\} dx,$$

where

$$\phi_{\alpha,\gamma_1^*}(x) := \frac{\alpha}{\gamma_1^{*\alpha+3}} \frac{\gamma_1^* + \alpha\gamma_1^* + \alpha\gamma_1^{*2} - \alpha(1 + \gamma_1^*)\log x}{x^{(\alpha+\gamma_1^*+\alpha\gamma_1^*)/\gamma_1^*}}. \quad (7.17)$$

This representation expresses the score as a linear functional of the Nelson–Aalen tail estimator.

Define the Nelson–Aalen tail product-limit process:

$$D_k(x) := \sqrt{k} \left\{ \frac{\bar{F}_n^{(NA)}(Z_{n-k:n}x)}{\bar{F}_n^{(NA)}(Z_{n-k:n})} - x^{-1/\gamma_1^*} \right\}, \text{ for } x > 1. \quad (7.18)$$

The asymptotic behavior of  $D_k(x)$  is the key ingredient for deriving the limit distribution.

### Step 2a: Gaussian approximation of $D_k(x)$

The key tool is the Gaussian approximation of the Nelson–Aalen tail process.

Recently, [Meraghni \*et al.\* \(2025\)](#) established such an approximation, which we now adopt.

Assume that the assumptions of Theorem 3.2 hold, with  $\sqrt{k}A_1(h) = O(1)$ , where  $h = h_n := U_H(n/k)$ .

Recall that  $U_H$  denotes the tail quantile function of  $H$ , and that  $A_1(h)$  appears in the second-order regular variation condition (3.13).

We also set  $q := 1 - p$ , where  $p$  is defined in (1.3) as the proportion of upper non-censored observations.

Then, there exists a sequence of standard Weiner processes  $\{W_n(s); 0 \leq s \leq 1\}$  defined on the common probability space  $(\Omega, \mathcal{A}, \mathbf{P})$ , such that, for  $p > 1/2$  and every  $0 < \epsilon < 1/2$ ,

$$\sup_{x \geq p^\gamma} x^{\epsilon/p\gamma_1} \left| D_k(x) - J_n(x) - x^{-1/\gamma_1} \frac{x^{\tau_1/\gamma_1} - 1}{\tau_1 \gamma_1} \sqrt{k}A_1(h) \right| \xrightarrow{\mathbf{P}} 0, \text{ as } n \rightarrow \infty, \quad (7.19)$$

where

$$J_n(x) = J_{n1}(x) + J_{n2}(x), \quad (7.20)$$

with

$$J_{1n}(x) := \sqrt{\frac{n}{k}} \left\{ x^{1/\gamma_2} \mathbf{W}_{n,1} \left( \frac{k}{n} x^{-1/\gamma} \right) - x^{-1/\gamma_1} \mathbf{W}_{n,1} \left( \frac{k}{n} \right) \right\},$$

and

$$J_{2n}(x) := \frac{x^{-1/\gamma_1}}{\gamma} \sqrt{\frac{n}{k}} \int_1^x u^{1/\gamma-1} \left\{ p \mathbf{W}_{n,2} \left( \frac{k}{n} u^{-1/\gamma} \right) - q \mathbf{W}_{n,1} \left( \frac{k}{n} u^{-1/\gamma} \right) \right\} du.$$

For each  $n$ ,  $\mathbf{W}_{n,1}(s)$  and  $\mathbf{W}_{n,2}(s)$  are independent centred Gaussian processes defined by:

$$\mathbf{W}_{n,1}(s) := \{W_n(\theta) - W_n(\theta - ps)\} \mathbb{I}_{\{\theta - ps \geq 0\}}$$

and

$$\mathbf{W}_{n,2}(s) := W_n(1) - W_n(1 - qs), \text{ for } 0 \leq s \leq 1.$$

This provides a precise stochastic decomposition of  $D_k(x)$  into a Gaussian component, a deterministic bias term, and a negligible remainder.

### Step 3: Decomposition of $\sqrt{k}\pi_k^{(1)}(\gamma_1^*)$ and asymptotic representation

Relying on Setp 2a, we can write

$$-\left(1 + \frac{1}{\alpha}\right)^{-1} \sqrt{k}\pi_k^{(1)}(\gamma_1^*) = \int_1^\infty \phi_{\alpha, \gamma_1^*}(x) D_k(x) dx := T_n.$$

Using the Gaussian approximation of  $D_k(x)$ , the term  $T_n$  naturally decomposes as

$$T_n = \underbrace{\int_1^\infty J_n(x) \phi_{\alpha, \gamma_1^*}(x) dx}_{\text{Gaussian term}} + \underbrace{\sqrt{k}A_1(h) \mu}_{\text{Asymptotic bias}} + \underbrace{R_n}_{\text{remainder}},$$

where

$$\mu := \int_1^\infty x^{-1/\gamma_1^*} \frac{x^{\tau_1/\gamma_1^*} - 1}{\gamma_1^* \tau_1} \phi_{\alpha, \gamma_1^*}(x) dx,$$

and

$$R_n := \int_1^\infty \left\{ D_k(x) - J_n(x) - x^{-1/\gamma_1^*} \frac{x^{\tau_1/\gamma_1^*} - 1}{\gamma_1^* \tau_1} \sqrt{k} A_1(h) \right\} \phi_{\alpha, \gamma_1^*}(x) dx.$$

The first term is Gaussian, since it is linear functional of the centred Gaussian processes  $\mathbf{W}_{n,1}(s)$  and  $\mathbf{W}_{n,2}(s)$ . By linearity of the integral, this mapping is linear, and hence Gaussian. Moreover, under the integrability assumptions on  $\phi_{\alpha, \gamma_1^*}(x)$  and the covariance structure of  $J_n(x)$ , the variance is finite and given explicitly in Proposition 8.2. The second term captures the asymptotic bias, while the third term is shown to be negligible.

Fix  $0 < \epsilon < 1$  and write

$$R_n = \int_1^\infty \left\{ x^{-\epsilon/p\gamma_1} \phi_{\alpha, \gamma_1^*}(x) \right\} x^{\epsilon/p\gamma_1} \left\{ D_k(x) - J_n(x) - x^{-1/\gamma_1^*} \frac{x^{\tau_1/\gamma_1^*} - 1}{\gamma_1^* \tau_1} \sqrt{k} A_1(h) \right\} dx.$$

It is straightforward to verify that  $\int_1^\infty x^{-\epsilon/p\gamma_1} |\phi_{\alpha, \gamma_1^*}(x)| dx$  is bounded by a finite linear combination of integrals of the form  $\int_1^\infty x^{-d} (\log x)^m dx$ ,  $m = 0, 1$ , for some  $d > 0$ . Hence by approximation (7.19),  $R_n = o_{\mathbf{P}}(1)$ , as  $n \rightarrow \infty$ . By elementary calculations, we obtain

$$\begin{aligned} \mu &:= \int_1^\infty x^{-1/\gamma_1^*} \frac{x^{\tau_1/\gamma_1^*} - 1}{\gamma_1^* \tau_1} \phi_{\alpha, \gamma_1^*}(x) dx \\ &= \frac{\alpha}{\tau_1 \gamma_1^{\alpha+2}} \frac{\tau_1 - 1}{\alpha - \tau_1 + \alpha \gamma_1 + 1} + \frac{\tau_1 \gamma_1^2 (2\alpha - \tau_1 + 2\alpha \gamma_1 + 2)}{(\alpha + \alpha \gamma_1 + 1)^2 (\alpha - \tau_1 + \alpha \gamma_1 + 1)^2}. \end{aligned} \quad (7.21)$$

Recalling that  $\sqrt{k} A_1(h) \rightarrow \lambda < 0$ , and using (7.16), we finally get

$$\left(1 + \frac{1}{\alpha}\right)^{-1} \eta^* \sqrt{k} (\hat{\gamma}_{1,\alpha} - \gamma_1^*) = \int_1^\infty J_n(x) \phi_{\alpha, \gamma_1^*}(x) dx + \lambda \mu + o_{\mathbf{P}}(1).$$

Since  $J_n(x)$  is centred, the integral term is centered as well. Therefore

$$\left(1 + \frac{1}{\alpha}\right)^{-1} \eta^* \sqrt{k} (\hat{\gamma}_{1,\alpha} - \gamma_1^*) \xrightarrow{\mathcal{D}} \mathcal{N}(\mu, \sigma^2), \text{ as } n \rightarrow \infty,$$

where  $\sigma^2$  is given in Proposition 8.2.

**7.3. Conclusion.** Combining Steps 1–3, we have shown that the properly normalized estimator  $\hat{\gamma}_{1,\alpha}$  decomposes into a centered Gaussian term, an explicit asymptotic bias, and a negligible remainder.

This completes the proof of Theorem 3.2.

## 8. Appendix A: Instrumental results

**Lemma 8.1.** *Under the assumptions of Theorem 3.1, we have*

$$-\left(1 + \frac{1}{\alpha}\right)^{-1} \pi_k^{(1)}(\gamma_1^*) = \int_1^\infty \phi_{\alpha, \gamma_1^*}(x) \left\{ \frac{\bar{F}_n^{(NA)}(Z_{n-k:n}x)}{\bar{F}_n^{(NA)}(Z_{n-k:n})} - x^{-1/\gamma_1^*} \right\} dx,$$

where  $\phi_{\alpha, \gamma_1^*}(x)$  is as in (7.17). Moreover  $\pi_k^{(1)}(\gamma_1^*) \xrightarrow{\mathbf{P}} 0$ , as  $n \rightarrow \infty$ .

*Proof.* We work under the conditions of Theorem 3.1, which assume that the cdfs  $F$  and  $G$  exhibit Pareto-type tail behavior with positive tail indices  $\gamma_1$  and  $\gamma_2$ , that the usual assumptions on the intermediate sequence  $k_n$  hold, and that the proportion  $p > 1/2$ .

Using the notations introduced in (7.14) and (7.15), we can write

$$-\pi_k^{(1)}(\gamma_1^*) = \left(1 + \frac{1}{\alpha}\right) A_{k, \alpha, \gamma_1^*}^{(1)} - \int_1^\infty \Psi_{\gamma_1^*, \alpha+1}^{(1)}(x) dx, \quad (8.22)$$

where

$$A_{k, \alpha, \gamma_1^*}^{(1)} = \sum_{i=1}^k \frac{\delta_{[n-i+1:n]}}{i} \frac{\bar{F}_n^{(NA)}(Z_{n-i+1:n})}{\bar{F}_n^{(NA)}(Z_{n-k:n})} \Psi_{\gamma_1^*, \alpha}^{(1)}\left(\frac{Z_{n-i+1:n}}{Z_{n-k:n}}\right),$$

and  $\bar{F}_n^{(NA)}$  denotes the Nelson-Aalen product-limit estimator of the cdf  $F$ , as defined in (1.4).

Furthermore,

$$\Psi_{\gamma_1^*, \alpha}^{(1)}(x) = \left. \frac{d\ell_{\gamma_1}^\alpha(x)}{d\gamma_1} \right|_{\gamma=\gamma_1^*} = \frac{\alpha}{\gamma_1^{*2+\alpha}} \frac{\log x - \gamma_1^*}{x^{\alpha(1+1/\gamma_1^*)}}.$$

Applying the representation (2.11), we may equivalently write:

$$A_{k, \alpha, \gamma_1^*}^{(1)} = \int_1^\infty \Psi_{\gamma_1^*, \alpha}^{(1)}(x) d\frac{\bar{F}_n^{(NA)}(Z_{n-k:n}x)}{\bar{F}_n^{(NA)}(Z_{n-k:n})}.$$

This may be rewritten as

$$A_{k, \alpha, \gamma_1^*}^{(1)} = - \int_1^\infty \phi_{\alpha, \gamma_1^*}(x) \frac{\bar{F}_n^{(NA)}(Z_{n-k:n}x)}{\bar{F}_n^{(NA)}(Z_{n-k:n})} dx, \quad (8.23)$$

where  $\phi_{\alpha, \gamma_1^*}(x) := d\Psi_{\gamma_1^*, \alpha}^{(1)}(x)/dx$ . On the other hand, by assertion (i) of Proposition 8.1, we have

$$\int_1^\infty \Psi_{\gamma_1^*, \alpha+1}^{(1)}(x) dx = - \left(1 + \frac{1}{\alpha}\right) \int_1^\infty \Psi_{\gamma_1^*, \alpha}^{(1)}(x) dx^{-1/\gamma_1^*}.$$

Applying integration by parts to the second integral gives

$$\int_1^\infty \Psi_{\gamma_1^*, \alpha}^{(1)}(x) dx^{-1/\gamma_1^*} = - \int_1^\infty \phi_{\alpha, \gamma_1^*}(x) x^{-1/\gamma_1^*} dx.$$

Therefore

$$\int_1^\infty \Psi_{\gamma_1^*, \alpha+1}^{(1)}(x) dx = \left(1 + \frac{1}{\alpha}\right) \int_1^\infty \phi_{\alpha, \gamma_1^*}(x) x^{-1/\gamma_1^*} dx. \quad (8.24)$$

Combining (8.22), (8.23) and (8.24), we obtain

$$-\left(1 + \frac{1}{\alpha}\right)^{-1} \pi_k^{(1)}(\gamma_1^*) = \int_1^\infty \phi_{\alpha, \gamma_1^*}(x) \left\{ \frac{\bar{F}_n^{(NA)}(Z_{n-k:n}x)}{\bar{F}_n^{(NA)}(Z_{n-k:n})} - x^{-1/\gamma_1^*} \right\} dx.$$

We decompose this integral as

$$I_{1n} := \int_1^\infty \phi_{\alpha, \gamma_1^*}(x) \left\{ \frac{\bar{F}_n^{(NA)}(Z_{n-k:n}x)}{\bar{F}_n^{(NA)}(Z_{n-k:n})} - \frac{\bar{F}(Z_{n-k:n}x)}{\bar{F}(Z_{n-k:n})} \right\} dx,$$

and

$$I_{2n} := \int_1^\infty \phi_{\alpha, \gamma_1^*}(x) \left\{ \frac{\bar{F}(Z_{n-k:n}x)}{\bar{F}(Z_{n-k:n})} - x^{-1/\gamma_1^*} \right\} dx.$$

For  $I_{1n}$ , using assertion (6.29) of [Meraghni et al. \(2025\)](#), there exists a sequence of Wiener processes  $\{W_n(s), 0 \leq s \leq 1\}$ , such for sufficiently small  $\eta, \epsilon_0 > 0$ ,

$$\sqrt{k} \left\{ \frac{\bar{F}_n^{(NA)}(Z_{n-k:n}x)}{\bar{F}_n^{(NA)}(Z_{n-k:n})} - \frac{\bar{F}(Z_{n-k:n}x)}{\bar{F}(Z_{n-k:n})} \right\} = J_n(x) + o_{\mathbf{P}}(1) x^{(2\eta-p)/\gamma+\epsilon_0},$$

uniformly for  $x \geq 1$ , where  $J_n(x)$  is a centered Gaussian process as defined: in (7.20). Consequently,

$$I_{1n} = o_{\mathbf{P}}(1) \int_1^\infty J_n(x) \phi_{\alpha, \gamma_1^*}(x) dx + o_{\mathbf{P}}(1) \int_1^\infty x^{(2\eta-p)/\gamma+\epsilon_0} \phi_{\alpha, \gamma_1^*}(x) dx.$$

Since  $\gamma_1 < \gamma_2$ , we have  $p > 1/2$  and thus  $(2\eta-p)/\gamma+\epsilon_0 < 0$ . The second integral is therefore finite, as it reduces to a linear combination of integrals of the form

$$\int_1^\infty x^{-d} (\log x)^j dx, \quad j = 0, 1,$$

for some  $d > 0$ . This implies that the second term in  $I_{1n}$  is  $o_{\mathbf{P}}(1)$ .

Next, we show that the expectation of the stochastic integral is also finite. Observe that

$$\mathbf{E} \left| \int_1^\infty J_n(x) \phi_{\alpha, \gamma_1^*}(x) dx \right| < \int_1^\infty \mathbf{E} |J_n(x)| |\phi_{\alpha, \gamma_1^*}(x)| dx. \quad (8.25)$$

Since  $\{W_n(s), 0 \leq s \leq 1\}$  is a sequence of Wiener processes, it follows that

$$\sqrt{\frac{n}{k}} \mathbf{E} \left| \mathbf{W}_{n,1} \left( \frac{k}{n} s \right) \right| \leq (ps)^{1/2} \quad \text{and} \quad \sqrt{\frac{n}{k}} \mathbf{E} \left| \mathbf{W}_{n,2} \left( \frac{k}{n} s \right) \right| \leq (qs)^{1/2},$$

where  $q := 1 - p$ . It follows that

$$\mathbf{E} |J_n(x)| = O(x^{1/(2\gamma_2)-1/(2\gamma_1)}),$$

uniformly for  $x > 1$ . Since  $\gamma_1 < \gamma_2$ , we have  $1/(2\gamma_2) - 1/(2\gamma_1) < 0$ , and therefore

$$\mathbf{E} |J_n(x)| = O(1),$$

uniformly for  $x > 1$ . On the other hand, we already established that

$$\int_1^\infty |\phi_{\alpha, \gamma_1^*}(x)| dx < \infty,$$

implying that the expectation in inequality (8.25) is finite. Hence, we conclude that  $I_{1n} = o_{\mathbf{P}}(1)$ . For  $I_{2n}$ , recall that

$$|I_{2n}| \leq \int_1^\infty \left| \frac{\bar{F}(Z_{n-k:n}x)}{\bar{F}(Z_{n-k:n})} - x^{-1/\gamma_1^*} \right| |\phi_{\alpha, \gamma_1^*}(x)| dx.$$

By assumption (1.2), the tail of  $F$  satisfies

$$\bar{F}(x) = x^{-1/\gamma_1^*} \ell_1(x),$$

where  $\ell_1(x)$  is a slowly varying function. Then, we can write

$$\frac{\bar{F}(Z_{n-k:n}x)}{\bar{F}(Z_{n-k:n})} - x^{-1/\gamma_1^*} = x^{-1/\gamma_1^*} \left\{ \frac{\ell_1(Z_{n-k:n}x)}{\ell_1(Z_{n-k:n})} - 1 \right\},$$

Applying Proposition B. 1.10 in [de Haan and Ferreira \(2006\)](#) (p. 369), for sufficiently small  $\epsilon > 0$ , we have uniformly for large  $Z_{n-k:n}$ ,

$$\left| \frac{\ell_1(Z_{n-k:n}x)}{\ell_1(Z_{n-k:n})} - 1 \right| \leq \epsilon x^\epsilon, \quad x > 1.$$

and thus

$$\left| \frac{\bar{F}(Z_{n-k:n}x)}{\bar{F}(Z_{n-k:n})} - x^{-1/\gamma_1^*} \right| \leq \epsilon x^{-1/\gamma_1^* + \epsilon}.$$

Consequently

$$|I_{2n}| \leq \epsilon \int_1^\infty x^{-1/\gamma_1^* + \epsilon} |\phi_{\alpha, \gamma_1^*}(x)| dx.$$

Since  $\phi_{\alpha, \gamma_1^*}(x)$  decays sufficiently fast and, for  $\epsilon > 0$ , can be chosen arbitrarily small, the above integral is finite. Therefore,

$$I_{2n} = o_{\mathbf{P}}(1).$$

Combining the two results, we conclude that

$$\pi_k^{(1)}(\gamma_1^*) = o_{\mathbf{P}}(1),$$

which completes the proof.  $\square$

**Lemma 8.2.** *Under the assumptions of Lemma 8.1, we have*

$$\pi_k^{(2)}(\gamma_1^*) \xrightarrow{\mathbf{P}} \eta^*, \quad \text{as } n \rightarrow \infty, \quad (8.26)$$

where

$$\eta^* := \frac{1 + \alpha}{\gamma_1^{*2+\alpha}} \frac{\alpha^2 (1 + \gamma_1^*)^2 + 1}{(\alpha (1 + \gamma_1^*) + 1)^3}. \quad (8.27)$$

*Proof.* In view of assertion (ii) of Proposition 8.1, we have the identity:

$$\int_1^\infty \Psi_{\gamma_1^*, \alpha+1}^{(2)}(x) dx = - \left( 1 + \frac{1}{\alpha} \right) \int_1^\infty \Psi_{\gamma_1^*, \alpha}^{(2)}(x) dx^{-1/\gamma_1^*} + \eta^*,$$

which implies that

$$\left( 1 + \frac{1}{\alpha} \right)^{-1} \left( \pi_k^{(2)}(\gamma_1^*) - \eta^* \right) = - \int_1^\infty \Psi_{\gamma_1^*, \alpha}^{(2)}(x) dx^{-1/\gamma_0} - A_{k, \alpha, \gamma_1^*}^{(2)}.$$

Following the same line of reasoning as in Lemma 8.1, we obtain

$$-\left(1 + \frac{1}{\alpha}\right)^{-1} \left(\pi_k^{(2)}(\gamma_1^*) - \eta^*\right) = \int_1^\infty \phi_{\alpha, \gamma_1^*}^{(2)}(x) \left\{ \frac{\bar{F}_n^{(NA)}(Z_{n-k:n}x)}{\bar{F}_n^{(NA)}(Z_{n-k:n})} - x^{-1/\gamma_1^*} \right\} dx,$$

where  $\phi_{\alpha, \gamma_1^*}^{(2)}(x) := d\Psi_{\gamma_1^*, \alpha}^{(2)}(x) / dx$ .

It is also straightforward to verify that

$$\int_1^\infty x^\epsilon \left| \phi_{\alpha, \gamma_1^*}^{(2)}(x) \right| dx < \infty,$$

for some  $\epsilon > 0$ . By applying Proposition 8.2, and the same arguments as in Lemma 8.1, we conclude that

$$\pi_k^{(2)}(\gamma_1^*) - \eta^* = o_{\mathbf{P}}(1),$$

which establishes the result.  $\square$

**Lemma 8.3.** *Given a sequence of rvs  $\tilde{\gamma}_1$  taking values in a neighborhood of  $\gamma_1^*$ , that is, such that for some  $\epsilon > 0$ ,  $|\tilde{\gamma}_1 - \gamma_1^*| \leq \epsilon$  with probability tending to one, it holds that*

$$\pi_k^{(3)}(\tilde{\gamma}_1) = O_{\mathbf{P}}(1), \text{ as } n \rightarrow \infty.$$

*Proof.* First, we show that  $\pi_k^{(3)}(\gamma_1^*) = O_{\mathbf{P}}(1)$ . Recall that

$$\begin{aligned} \pi_k^{(3)}(\gamma_1^*) &= \int_1^\infty \Psi_{\gamma_1^*, \alpha+1}^{(3)}(x) dx \\ &\quad - (1 + 1/\alpha) \sum_{i=1}^k \frac{\delta_{[n-i+1:n]}}{i} \frac{\bar{F}_n^{(NA)}(Z_{n-i+1:n})}{\bar{F}_n^{(NA)}(Z_{n-k:n})} \Psi_{\gamma_1^*, \alpha}^{(3)}\left(\frac{Z_{n-i+1:n}}{Z_{n-k:n}}\right). \end{aligned}$$

By Proposition 8.2, we can rewrite this as

$$\pi_k^{(3)}(\gamma_1^*) = \left(1 + \frac{1}{\alpha}\right) A_{k, \alpha, \gamma_1^*}^{(3)} + \zeta^*,$$

where

$$A_{k, \alpha, \gamma_1^*}^{(3)} := - \int_1^\infty \Psi_{\gamma_1^*, \alpha}^{(3)}(x) dx^{-1/\gamma_1^*} - \sum_{i=1}^k \frac{\delta_{[n-i+1:n]}}{i} \frac{\bar{F}_n^{(NA)}(Z_{n-i+1:n})}{\bar{F}_n^{(NA)}(Z_{n-k:n})} \Psi_{\gamma_1^*, \alpha}^{(3)}\left(\frac{Z_{n-i+1:n}}{Z_{n-k:n}}\right).$$

Using arguments similar to Lemma 8.2, we can show that  $A_{k, \alpha, \gamma_1^*}^{(3)} \xrightarrow{\mathbf{P}} 0$ . Hence  $\pi_k^{(3)}(\gamma_1^*) \xrightarrow{\mathbf{P}} \zeta^* < \infty$ , implying  $\pi_k^{(3)}(\gamma_1^*) = O_{\mathbf{P}}(1)$ . Next, we prove that  $\pi_k^{(3)}(\tilde{\gamma}_1) - \pi_k^{(3)}(\gamma_1^*) = O_{\mathbf{P}}(1)$ , as

$n \rightarrow \infty$ . Indeed, write

$$\begin{aligned} & \pi_k^{(3)}(\tilde{\gamma}_1) - \pi_k^{(3)}(\gamma_1^*) \\ &= \int_1^\infty \left\{ \Psi_{\tilde{\gamma}_1, \alpha+1}^{(3)}(x) - \Psi_{\gamma_1^*, \alpha+1}^{(3)}(x) \right\} dx \\ &\quad - (1 + 1/\alpha) \sum_{i=1}^k \frac{\delta_{[n-i+1:n]}}{i} \frac{\bar{F}_n^{(NA)}(Z_{n-i+1:n})}{\bar{F}_n^{(NA)}(Z_{n-k:n})} \\ &\quad \times \left\{ \Psi_{\tilde{\gamma}_1, \alpha}^{(3)}\left(\frac{Z_{n-i+1:n}}{Z_{n-k:n}}\right) - \Psi_{\gamma_1^*, \alpha}^{(3)}\left(\frac{Z_{n-i+1:n}}{Z_{n-k:n}}\right) \right\}. \end{aligned}$$

By the mean value theorem, there exists a value  $\bar{\gamma}_1$  lying between  $\tilde{\gamma}_1$  and  $\gamma_1^*$  such that

$$\int_1^\infty \left\{ \Psi_{\tilde{\gamma}_1, \alpha+1}^{(3)}(x) - \Psi_{\gamma_1^*, \alpha+1}^{(3)}(x) \right\} dx = (\tilde{\gamma}_1 - \gamma_1^*) \int_1^\infty \frac{d^4}{d\gamma^4} \ell_{\bar{\gamma}_1}^{\alpha+1}(x) dx.$$

From Proposition 8.2 in [Mancer et al. \(2025\)](#), the integral on the right-hand side is stochastically finite. Since  $\tilde{\gamma}_1$  lies in a neighborhood of  $\gamma_1^*$ ,  $\tilde{\gamma}_1 - \gamma_1^* = O_{\mathbf{P}}(1)$ , and therefore the integral difference is  $O_{\mathbf{P}}(1)$ .

Similarly, the summation term can be expressed as a Stieltjes integral:

$$\begin{aligned} & \sum_{i=1}^k \frac{\delta_{[n-i+1:n]}}{i} \frac{\bar{F}_n^{(NA)}(Z_{n-i+1:n})}{\bar{F}_n^{(NA)}(Z_{n-k:n})} \left\{ \Psi_{\tilde{\gamma}_1, \alpha}^{(3)}\left(\frac{Z_{n-i+1:n}}{Z_{n-k:n}}\right) - \Psi_{\gamma_1^*, \alpha+1}^{(3)}\left(\frac{Z_{n-i+1:n}}{Z_{n-k:n}}\right) \right\} \\ &= \int_1^\infty \left\{ \Psi_{\tilde{\gamma}_1, \alpha}^{(3)}(x) - \Psi_{\gamma_1^*, \alpha+1}^{(3)}(x) \right\} d\frac{\bar{F}_n^{(NA)}(Z_{n-k:n}x)}{\bar{F}_n^{(NA)}(Z_{n-k:n})}. \end{aligned}$$

Applying the mean value theorem and integration by parts, this integral is also

$$(\tilde{\gamma}_1 - \gamma_1^*) \int_1^\infty \Psi_{\bar{\gamma}_1, \alpha}^{(4)}(x) d\frac{\bar{F}_n^{(NA)}(Z_{n-k:n}x)}{\bar{F}_n^{(NA)}(Z_{n-k:n})},$$

where  $\bar{\gamma}_1$  lies between  $\tilde{\gamma}_1$  and  $\gamma_1^*$ . By an integration by parts, we obtain

$$\begin{aligned} & \int_1^\infty \Psi_{\bar{\gamma}_1, \alpha}^{(4)}(x) d\frac{\bar{F}_n^{(NA)}(Z_{n-k:n}x)}{\bar{F}_n^{(NA)}(Z_{n-k:n})} \\ &= \Psi_{\bar{\gamma}_1, \alpha}^{(4)}(1) - \int_1^\infty \left\{ \frac{\bar{F}_n^{(NA)}(Z_{n-k:n}x)}{\bar{F}_n^{(NA)}(Z_{n-k:n})} - \frac{\bar{F}(Z_{n-k:n}x)}{\bar{F}(Z_{n-k:n})} \right\} \phi_{\alpha, \bar{\gamma}_1}^{(4)}(x) dx \\ &\quad + \int_1^\infty \left\{ \frac{\bar{F}(Z_{n-k:n}x)}{\bar{F}(Z_{n-k:n})} - x^{-1/\gamma_1} \right\} \phi_{\alpha, \bar{\gamma}_1}^{(4)}(x) dx + \int_1^\infty x^{-1/\gamma_1} \phi_{\alpha, \bar{\gamma}_1}^{(4)}(x) dx, \end{aligned}$$

where  $\phi_{\alpha, \bar{\gamma}_1}^{(4)}(x) := d\Psi_{\bar{\gamma}_1, \alpha}^{(4)}(x)/dx$ . By arguments similar to those used earlier, the first, and fourth terms are  $O_{\mathbf{P}}(1)$  while the second and third terms are  $o_{\mathbf{P}}(1)$ . Hence, the integral is  $O_{\mathbf{P}}(1)$ .

Since for a fixed  $\epsilon > 0$ ,  $|\tilde{\gamma}_1 - \gamma_1^*| \leq \epsilon$ , it follows that  $\tilde{\gamma}_1 - \gamma_1^* = O_{\mathbf{P}}(1)$ . We conclude that

$$\pi_k^{(3)}(\tilde{\gamma}_1) - \pi_k^{(3)}(\gamma_1^*) = O_{\mathbf{P}}(1),$$

which finally implies that

$$\pi_k^{(3)}(\tilde{\gamma}_1) = O_{\mathbf{P}}(1)$$

as claimed.  $\square$

**Proposition 8.1.** *For any  $\alpha > 0$ , the following identities hold.*

- (i)  $\int_1^\infty \Psi_{\gamma_1^*, \alpha+1}^{(1)}(x) dx = -\left(1 + \frac{1}{\alpha}\right) \int_1^\infty \Psi_{\gamma_1^*, \alpha}^{(1)}(x) dx.$
- (ii)  $\int_1^\infty \Psi_{\gamma_1^*, \alpha+1}^{(2)}(x) dx = -\left(1 + \frac{1}{\alpha}\right) \int_1^\infty \Psi_{\gamma_1^*, \alpha}^{(2)}(x) dx^{-1/\gamma_1^*} + \eta^*,$   
where  $\eta^* > 0$  is as in (8.27).
- (iii)  $\int_1^\infty \Psi_{\gamma_1^*, \alpha+1}^{(3)}(x) dx = -\left(1 + \frac{1}{\alpha}\right) \int_1^\infty \Psi_{\gamma_1^*, \alpha}^{(3)}(x) dx^{-1/\gamma_1^*} + \zeta^*,$   
where  $\zeta^*$  denotes a finite constant.

*Proof.* Let  $J$  be continuous, nonincreasing, and nonnegative on  $(0, 1)$ , and satisfies  $\int_0^1 J(s) ds = 1$ . From Proposition 8.1 of [Mancer et al. \(2025\)](#), for every  $\alpha > 0$ , we have

$$\begin{aligned} \Psi_{\gamma_1^*, \alpha+1}^{(1)}(x) &= (1 + 1/\alpha) \ell_{\gamma_1^*, J}(x) \Psi_{\gamma_1^*, \alpha}^{(1)}(x), \\ \Psi_{\gamma_1^*, \alpha+1}^{(2)}(x) &= (1 + 1/\alpha) \ell_{\gamma_1^*, J}(x) \Psi_{\gamma_1^*, \alpha}^{(2)}(x) + (1 + \alpha) \left( \Psi_{\gamma_1^*, 1}^{(1)}(x) \right)^2 \ell_{\gamma_1^*, J}^{\alpha-1}(x), \\ \Psi_{\gamma_1^*, \alpha+1}^{(3)}(x) &= (1 + 1/\alpha) \ell_{\gamma_1^*, J}(x) \Psi_{\gamma_1^*, \alpha}^{(3)}(x) + g_{\gamma_1^*, \alpha}(x), \end{aligned}$$

for some integrable function  $x \mapsto g_{\gamma_1^*, \alpha}(x)$ , where

$$\ell_{\gamma_1^*, J}(x) := J(x^{-1/\gamma_1^*}) \ell_{\gamma_1^*}(x), \quad x > 1.$$

Integrating each equality over  $(1, \infty)$  yields the identities in Proposition 8.1, with

$$0 < \eta^* = (1 + \alpha) \int_1^\infty \left( \Psi_{\gamma_1^*, 1}^{(1)}(x) \right)^2 \ell_{\gamma_1^*}^{\alpha-1}(x) dx < \infty, \quad \zeta^* = \int_1^\infty g_{\gamma_1^*, \alpha}(x) dx < \infty.$$

In the present paper, we take  $J(x) = 1$ , which reduces  $\ell_{\gamma_1^*, J}(x)$  to  $\ell_{\gamma_1^*}(x)$ . This choice trivially satisfies all the above regularity conditions, so the identities remain valid for the strict Pareto law. This completes the proof of Proposition 8.1.  $\square$

**Proposition 8.2.** *The asymptotic variance*

$$\begin{aligned} \sigma^2 := & \int_1^\infty \int_1^\infty \min(x^{-1/\gamma^*}, y^{-1/\gamma^*}) K(x, y) dx dy \\ & - 2 \int_1^\infty x^{-1/\gamma^*} \Delta_1(x) dx + p \left( \int_1^\infty x^{-1/\gamma_1^*} \phi_{\alpha, \gamma_1^*}(x) dx \right)^2, \end{aligned} \tag{8.28}$$

where

$$\begin{aligned} K(x, y) &:= p\Delta_1(x)\Delta_1(y) + \frac{q}{\gamma_1^*}\Delta_2(x)\Delta_2(y), \\ \Delta_1(x) &:= x^{q/\gamma^*}\phi_{\alpha, \gamma_1^*}(x) - qx^{1/\gamma^*}V(x), \quad \Delta_2(x) := x^{1/\gamma^*}V(x), \\ V(x) &:= \int_x^\infty t^{-1/\gamma_1^*}\phi_{\alpha, \gamma_1^*}(t) dt. \end{aligned}$$

Here  $\phi_{\alpha, \gamma_1^*}$  is defined in 7.17. Moreover,  $\gamma^*$  and  $\gamma_1^*$  denote the true values of the tail indices  $\gamma$  and  $\gamma_1$  associated with the cdfs  $\bar{H}$  and  $\bar{F}$  respectively.

*Proof.* Recalling that  $q = 1 - p$  and  $\gamma_2^* = \gamma^*/q$ , and the expression of  $J_n(x)$  given in (7.20), we decompose

$$\mathbb{I}_n := \int_1^\infty J_n(x)\phi_{\alpha, \gamma_1^*}(x) dx = \mathbb{I}_{n1} + \mathbb{I}_{n2},$$

where

$$\mathbb{I}_{n1} := \int_1^\infty J_{n1}(x)\phi_{\alpha, \gamma_1^*}(x) dx \text{ and } \mathbb{I}_{n2} := \int_1^\infty J_{n2}(x)\phi_{\alpha, \gamma_1^*}(x) dx.$$

with

$$J_{1n}(x) := \sqrt{\frac{n}{k}} \left\{ x^{q/\gamma^*} \mathbf{W}_{n,1} \left( \frac{k}{n} x^{-1/\gamma^*} \right) - x^{-1/\gamma_1^*} \mathbf{W}_{n,1} \left( \frac{k}{n} \right) \right\},$$

and

$$J_{2n}(x) := \frac{x^{-1/\gamma_1^*}}{\gamma^*} \sqrt{\frac{n}{k}} \int_1^x u^{1/\gamma^*-1} \left\{ p \mathbf{W}_{n,2} \left( \frac{k}{n} u^{-1/\gamma^*} \right) - q \mathbf{W}_{n,1} \left( \frac{k}{n} u^{-1/\gamma^*} \right) \right\} du.$$

It is straightforward to verify that

$$\mathbb{I}_{n1} = \sqrt{\frac{n}{k}} \int_1^\infty x^{q/\gamma^*} W_{n,1} \left( \frac{k}{n} x^{-1/\gamma^*} \right) \phi_{\alpha, \gamma_1^*}(x) dx - a \sqrt{\frac{n}{k}} W_{n,1} \left( \frac{k}{n} \right),$$

where  $a := \int_1^\infty x^{-q/\gamma^*} \phi_{\alpha, \gamma_1^*}(x) dx$ . Integrating  $\mathbb{I}_{n2}$  by parts, yields

$$\mathbb{I}_{n2} = \frac{1}{\gamma_1^*} \sqrt{\frac{n}{k}} \int_1^\infty x^{q/\gamma^*} \left\{ p W_{n,2} \left( \frac{k}{n} x^{-1/\gamma^*} \right) - q W_{n,1} \left( \frac{k}{n} x^{-1/\gamma^*} \right) \right\} V(x) dx.$$

Hence,  $\mathbb{I}_n$  can be rewritten as

$$\begin{aligned} \mathbb{I}_{n1} &= \sqrt{\frac{n}{k}} \int_1^\infty W_{n,1} \left( \frac{k}{n} x^{-1/\gamma_1^*} \right) \Delta_1(x) dx - a \sqrt{\frac{n}{k}} W_{n,1} \left( \frac{k}{n} \right), \\ \mathbb{I}_{n2} &= \frac{1}{\gamma_1^*} \sqrt{\frac{n}{k}} \int_1^\infty W_{n,2} \left( \frac{k}{n} x^{-1/\gamma^*} \right) \Delta_2(x) dx. \end{aligned}$$

Since  $W_{n,1}$  and  $W_{n,2}$  are centered and independent Gaussian processes, the rvs  $\mathbb{I}_{n1}$ ,  $\mathbb{I}_{n2}$ , and their product  $\mathbb{I}_{n1} \times \mathbb{I}_{n2}$  are centered. Taking expectations, we obtain

$$\begin{aligned} \mathbf{E}[\mathbb{I}_{n1}^2] &= p \int_1^\infty \int_1^\infty \min(x^{-1/\gamma^*}, y^{-1/\gamma^*}) \Delta_1(x)\Delta_1(y) dx dy + pa^2 - 2 \int_1^\infty x^{-1/\gamma^*} \Delta_1(x) dx, \\ \mathbf{E}[\mathbb{I}_{n2}^2] &= \frac{q}{\gamma_1^*} \int_1^\infty \int_1^\infty \min(x^{-1/\gamma_1^*}, y^{-1/\gamma_1^*}) \Delta_2(x)\Delta_2(y) dx dy, \end{aligned}$$

The sum of these two expressions yields the asymptotic variance formula  $\sigma^2$  given in (8.28), which completes the proof.  $\square$

## 9. Appendix B: Simulation results

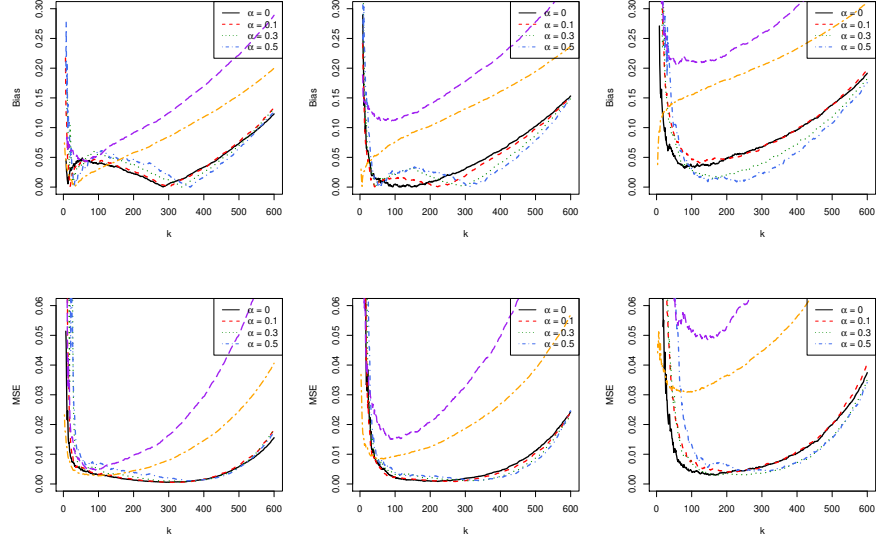


FIGURE 9.1. Bias (top panel) and MSE (bottom panel) of the MDPD tail index estimator  $\hat{\gamma}_{1,\alpha}$ , together with  $\hat{\gamma}_1^{(EFG)}$  (long-dashed purple line) and  $\hat{\gamma}_1^{(W)}$  (two-dashed orange line) computed from 2000 Monte Carlo samples of size 1000 generated from Scenario **S1**, with  $\gamma_1 = 0.3$ ,  $\gamma_c = 0.6$  and  $p = 0.55$ . Contamination is introduced before the censoring mechanism, with  $\epsilon = 0$  (left panel),  $\epsilon = 0.15$  (middle panel), and  $\epsilon = 0.40$  (right panel).

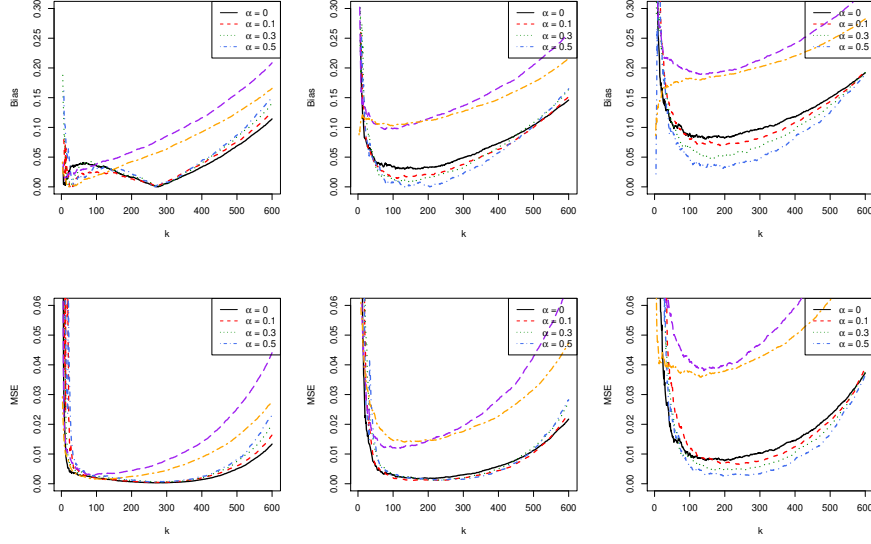


FIGURE 9.2. Bias (top panel) and MSE (bottom panel) of the MDPD tail index estimator  $\hat{\gamma}_{1,\alpha}$ , together with  $\hat{\gamma}_1^{(EFG)}$  (long-dashed purple line) and  $\hat{\gamma}_1^{(W)}$  (two-dashed orange line) computed from 2000 Monte Carlo samples of size 1000 generated from Scenario **S1**, with  $\gamma_1 = 0.3$ ,  $\gamma_c = 0.6$  and  $p = 0.7$ . Contamination is introduced before the censoring mechanism, with  $\epsilon = 0$  (left panel),  $\epsilon = 0.15$  (middle panel), and  $\epsilon = 0.40$  (right panel).

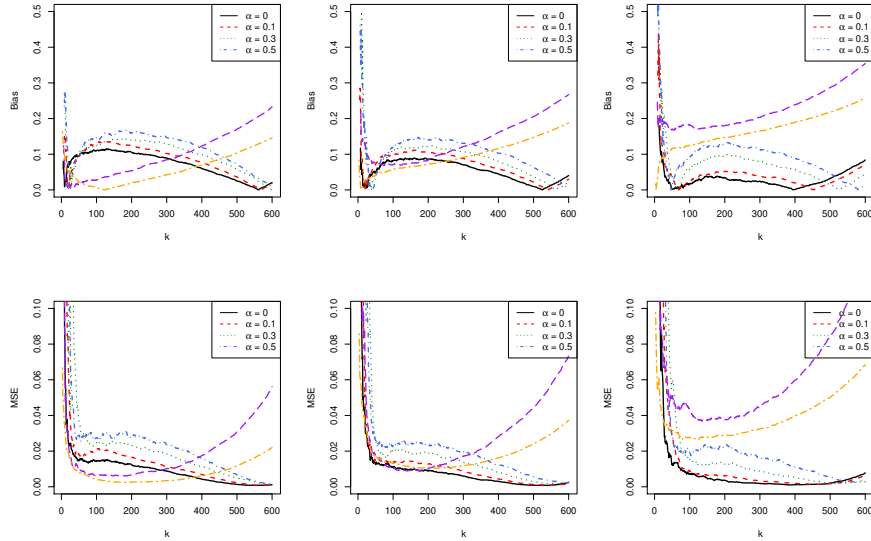


FIGURE 9.3. Bias (top panel) and MSE (bottom panel) of the MDPD tail index estimator  $\hat{\gamma}_{1,\alpha}$ , together with  $\hat{\gamma}_1^{(EFG)}$  (long-dashed purple line) and  $\hat{\gamma}_1^{(W)}$  (two-dashed orange line) computed from 2000 Monte Carlo samples of size 1000 generated from Scenario **S1**, with  $\gamma_1 = 0.5$ ,  $\gamma_c = 0.8$  and  $p = 0.55$ . Contamination is introduced before the censoring mechanism, with  $\epsilon = 0$  (left panel),  $\epsilon = 0.15$  (middle panel), and  $\epsilon = 0.40$  (right panel).

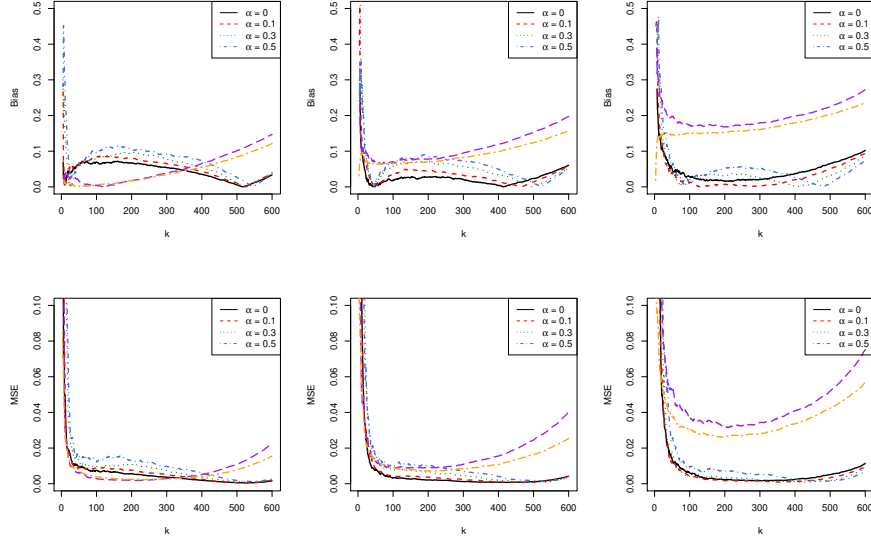


FIGURE 9.4. Bias (top panel) and MSE (bottom panel) of the MDPD tail index estimator  $\hat{\gamma}_{1,\alpha}$ ,  $\hat{\gamma}_1^{(EFG)}$  (longdashed purple line) and  $\hat{\gamma}_1^{(W)}$  (twodashed orange line) based on 2000 samples of size 1000 from scenario **S1**, for  $\gamma_1 = 0.5$ ,  $\gamma_c = 0.8$  and  $p = 0.7$ , under contamination introduced before the censoring mechanism, with  $\epsilon = 0$  (left panel),  $\epsilon = 0.15$  (middle panel) and  $\epsilon = 0.40$  (right panel).

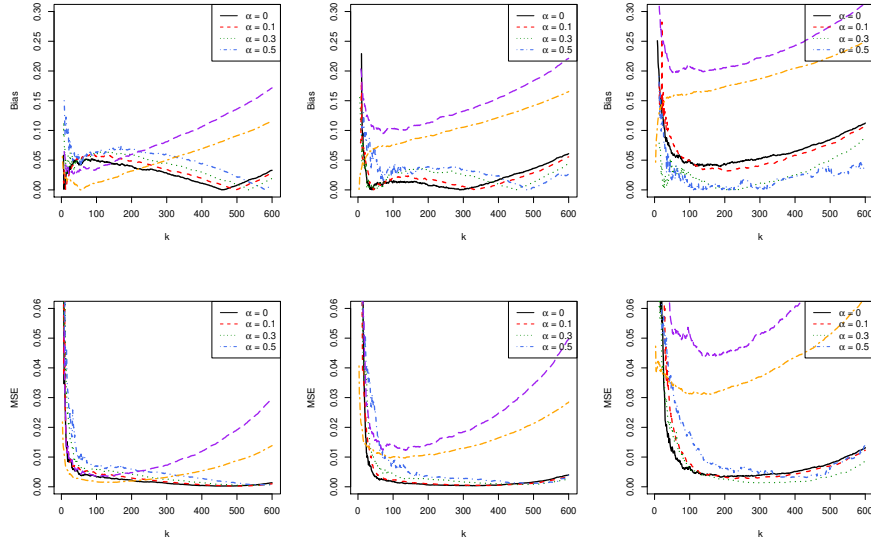


FIGURE 9.5. Bias (top panel) and MSE (bottom panel) of the MDPD tail index estimator  $\hat{\gamma}_{1,\alpha}$ , together with  $\hat{\gamma}_1^{(EFG)}$  (long-dashed purple line) and  $\hat{\gamma}_1^{(W)}$  (two-dashed orange line) computed from 2000 Monte Carlo samples of size 1000 generated from Scenario **S2**, with  $\gamma_1 = 0.3$ ,  $\gamma_c = 0.6$  and  $p = 0.55$ . Contamination is introduced before the censoring mechanism, with  $\epsilon = 0$  (left panel),  $\epsilon = 0.15$  (middle panel), and  $\epsilon = 0.40$  (right panel).

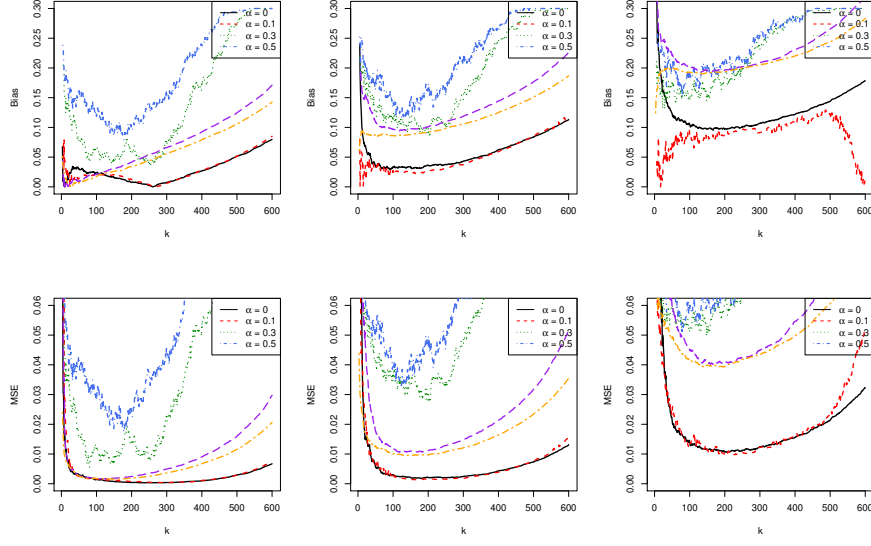


FIGURE 9.6. Bias (top) and MSE (bottom) of the MDPD tail index estimator  $\hat{\gamma}_{1,\alpha}$ , together with  $\hat{\gamma}_1^{(EFG)}$  (long-dashed purple line) and  $\hat{\gamma}_1^{(W)}$  (two-dashed orange line) computed from 2000 Monte Carlo samples of size 1000 generated from Scenario **S2**, with  $\gamma_1 = 0.3$ ,  $\gamma_c = 0.6$  and  $p = 0.7$ . Contamination is introduced before the censoring mechanism, with  $\epsilon = 0$  (left panel),  $\epsilon = 0.15$  (middle panel), and  $\epsilon = 0.40$  (right panel).

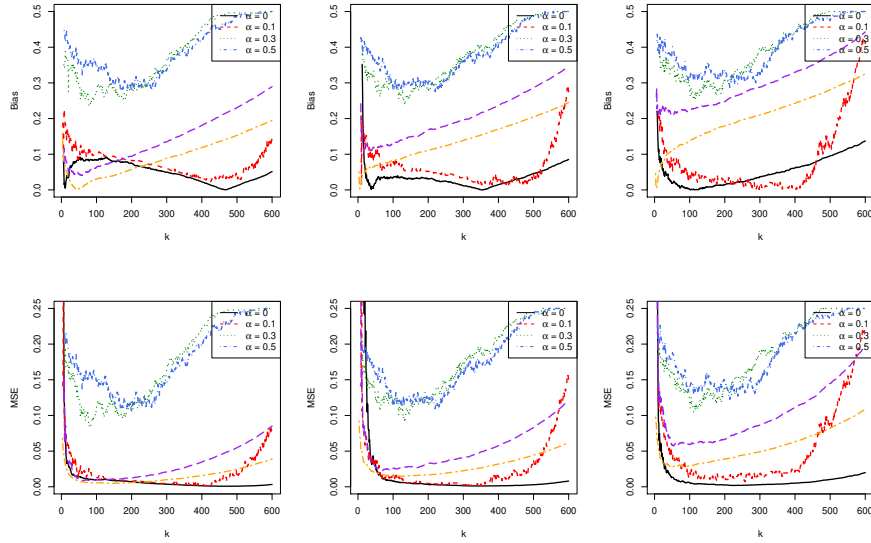


FIGURE 9.7. Bias (top panel) and MSE (bottom panel) of the MDPD tail index estimator  $\hat{\gamma}_{1,\alpha}$ , together with  $\hat{\gamma}_1^{(EFG)}$  (long-dashed purple line) and  $\hat{\gamma}_1^{(W)}$  (two-dashed orange line) computed from 2000 Monte Carlo samples of size 1000 generated from Scenario **S2**, with  $\gamma_1 = 0.5$ ,  $\gamma_c = 0.8$  and  $p = 0.55$ . Contamination is introduced before the censoring mechanism, with  $\epsilon = 0$  (left panel),  $\epsilon = 0.15$  (middle panel), and  $\epsilon = 0.40$  (right panel).

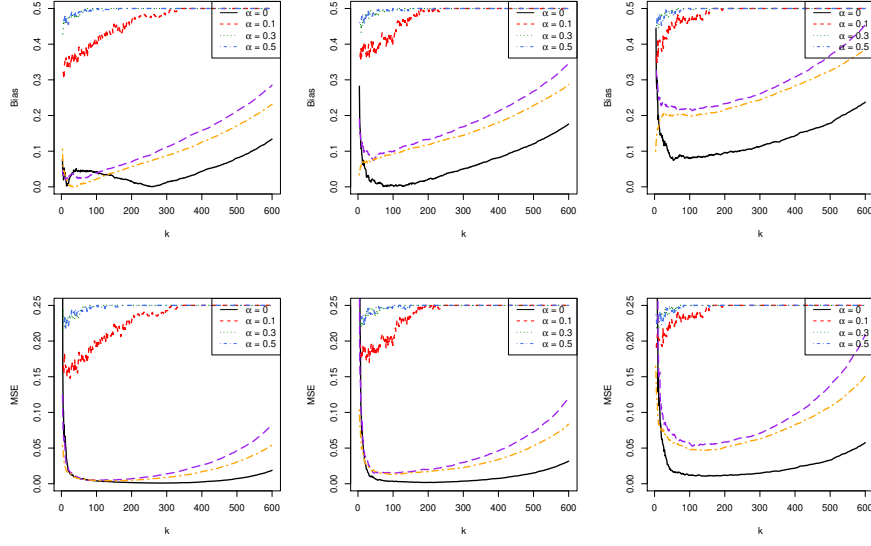


FIGURE 9.8. Bias (top panel) and MSE (bottom panel) of the MDPD tail index estimator  $\hat{\gamma}_{1,\alpha}$ , together with  $\hat{\gamma}_1^{(EFG)}$  (long-dashed purple line) and  $\hat{\gamma}_1^{(W)}$  (two-dashed orange line) computed from 2000 Monte Carlo samples of size 1000 generated from Scenario **S2**, with  $\gamma_1 = 0.5$ ,  $\gamma_c = 0.8$  and  $p = 0.7$ . Contamination is introduced before the censoring mechanism, with  $\epsilon = 0$  (left panel),  $\epsilon = 0.15$  (middle panel), and  $\epsilon = 0.40$  (right panel).

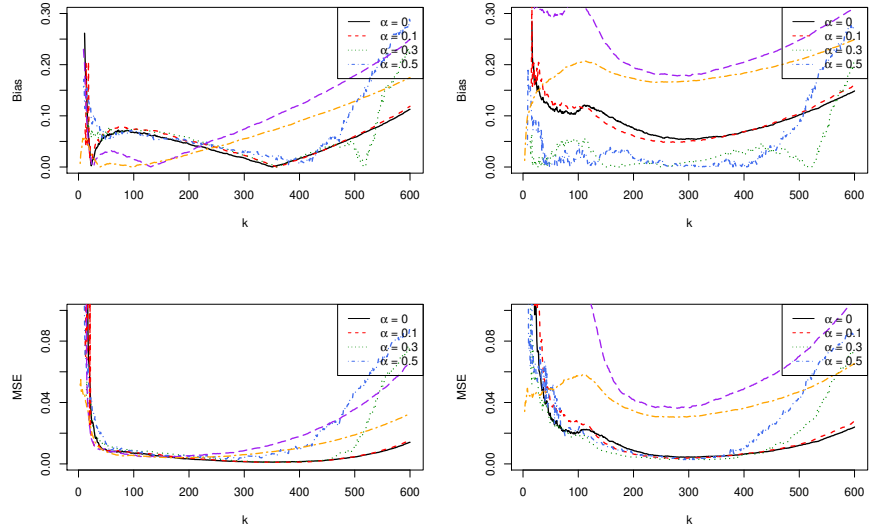


FIGURE 9.9. Bias (top panel) and MSE (bottom panel) of the MDPD tail index estimator  $\hat{\gamma}_{1,\alpha}$ , together with  $\hat{\gamma}_1^{(EFG)}$  (long-dashed purple line) and  $\hat{\gamma}_1^{(W)}$  (two-dashed orange line) computed from 2000 Monte Carlo samples of size 1000 generated from Scenario **S1**, with  $\gamma_1 = 0.3$ ,  $\gamma_c = 0.6$  and  $p = 0.55$ . Contamination is introduced after the censoring mechanism, with  $\epsilon = 0$  (left panel),  $\epsilon = 0.15$  (middle panel), and  $\epsilon = 0.40$  (right panel).

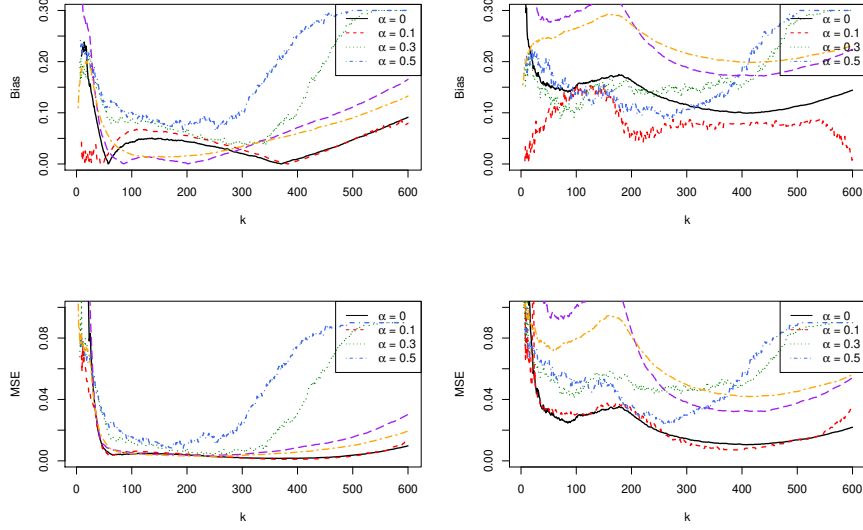


FIGURE 9.10. Bias (top panel) and MSE (bottom panel) of the MDPD tail index estimator  $\hat{\gamma}_{1,\alpha}$ , together with  $\hat{\gamma}_1^{(EFG)}$  (long-dashed purple line) and  $\hat{\gamma}_1^{(W)}$  (two-dashed orange line) computed from 2000 Monte Carlo samples of size 1000 generated from Scenario **S1**, with  $\gamma_1 = 0.3$ ,  $\gamma_c = 0.6$  and  $p = 0.7$ . Contamination is introduced after the censoring mechanism, with  $\epsilon = 0$  (left panel),  $\epsilon = 0.15$  (middle panel), and  $\epsilon = 0.40$  (right panel).

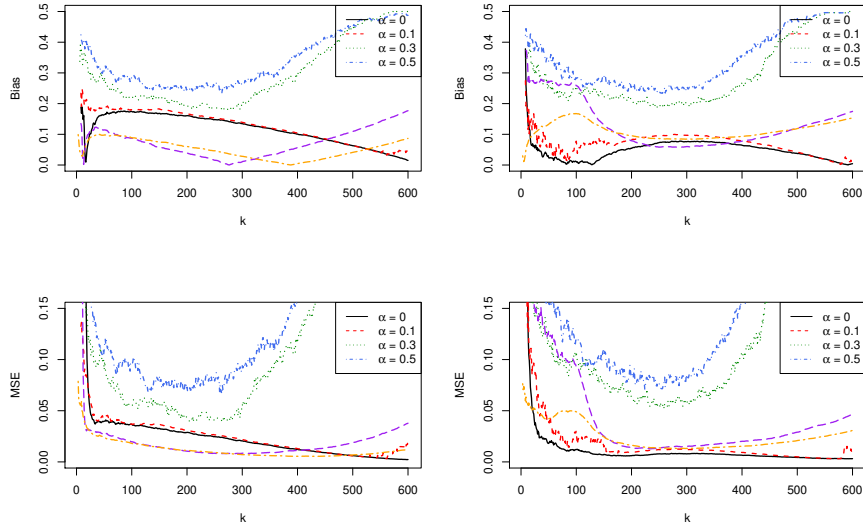


FIGURE 9.11. Bias (top panel) and MSE (bottom panel) of the MDPD tail index estimator  $\hat{\gamma}_{1,\alpha}$ , together with  $\hat{\gamma}_1^{(EFG)}$  (long-dashed purple line) and  $\hat{\gamma}_1^{(W)}$  (two-dashed orange line) computed from 2000 Monte Carlo samples of size 1000 generated from Scenario **S1**, with  $\gamma_1 = 0.5$ ,  $\gamma_c = 0.8$  and  $p = 0.55$ . Contamination is introduced after the censoring mechanism, with  $\epsilon = 0$  (left panel),  $\epsilon = 0.15$  (middle panel), and  $\epsilon = 0.40$  (right panel).

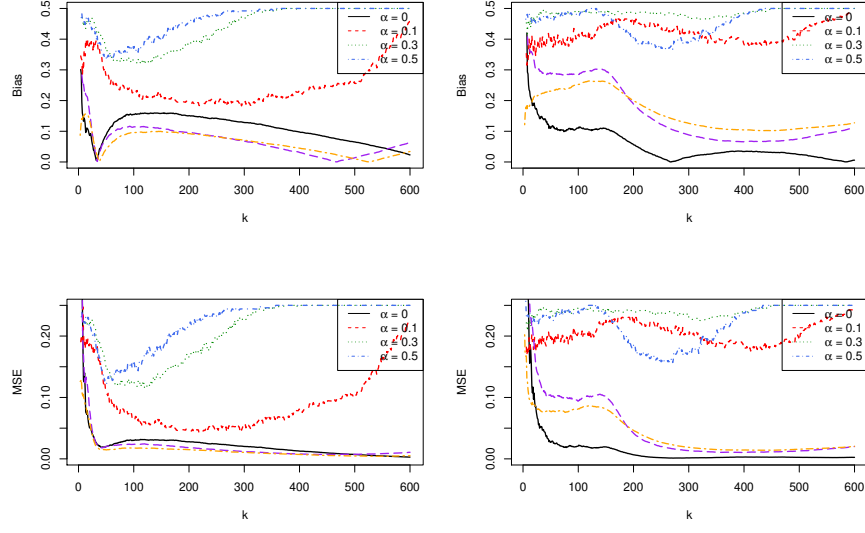


FIGURE 9.12. Bias (top panel) and MSE (bottom panel) of the MDPD tail index estimator  $\hat{\gamma}_{1,\alpha}$ , together with  $\hat{\gamma}_1^{(EFG)}$  (long-dashed purple line) and  $\hat{\gamma}_1^{(W)}$  (two-dashed orange line) computed from 2000 Monte Carlo samples of size 1000 generated from Scenario **S1**, with  $\gamma_1 = 0.5$ ,  $\gamma_c = 0.8$  and  $p = 0.7$ . Contamination is introduced after the censoring mechanism, with  $\epsilon = 0$  (left panel),  $\epsilon = 0.15$  (middle panel), and  $\epsilon = 0.40$  (right panel).

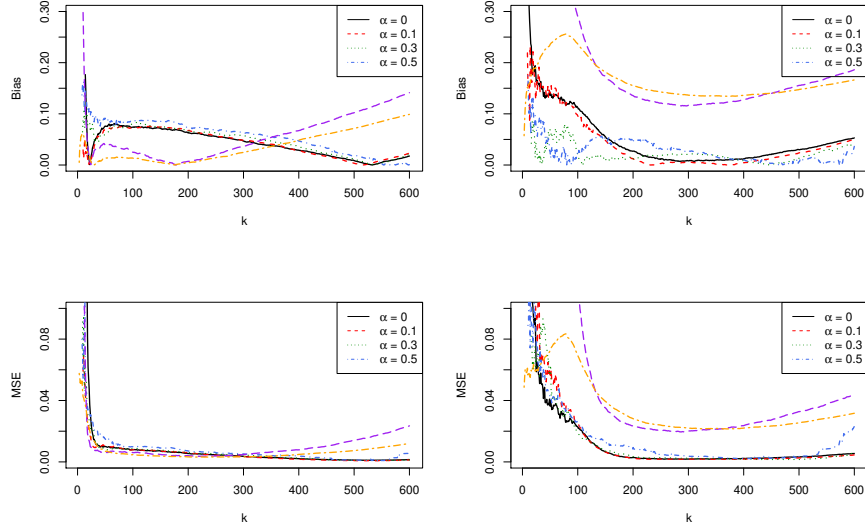


FIGURE 9.13. Bias (top panel) and MSE (bottom panel) of the MDPD tail index estimator  $\hat{\gamma}_{1,\alpha}$ , together with  $\hat{\gamma}_1^{(EFG)}$  (long-dashed purple line) and  $\hat{\gamma}_1^{(W)}$  (two-dashed orange line) computed from 2000 Monte Carlo samples of size 1000 generated from Scenario **S2**, with  $\gamma_1 = 0.3$ ,  $\gamma_c = 0.6$  and  $p = 0.55$ . Contamination is introduced after the censoring mechanism, with  $\epsilon = 0$  (left panel),  $\epsilon = 0.15$  (middle panel), and  $\epsilon = 0.40$  (right panel).

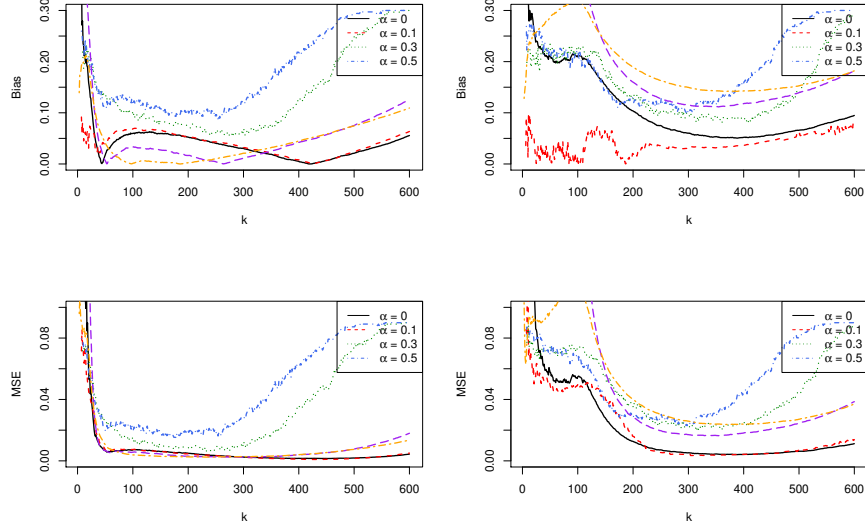


FIGURE 9.14. Bias (top panel) and MSE (bottom panel) of the MDPD tail index estimator  $\hat{\gamma}_{1,\alpha}$ , together with  $\hat{\gamma}_1^{(EFG)}$  (long-dashed purple line) and  $\hat{\gamma}_1^{(W)}$  (two-dashed orange line) computed from 2000 Monte Carlo samples of size 1000 generated from Scenario **S2**, with  $\gamma_1 = 0.3$ ,  $\gamma_c = 0.6$  and  $p = 0.7$ . Contamination is introduced after the censoring mechanism, with  $\epsilon = 0$  (left panel),  $\epsilon = 0.15$  (middle panel), and  $\epsilon = 0.40$  (right panel).

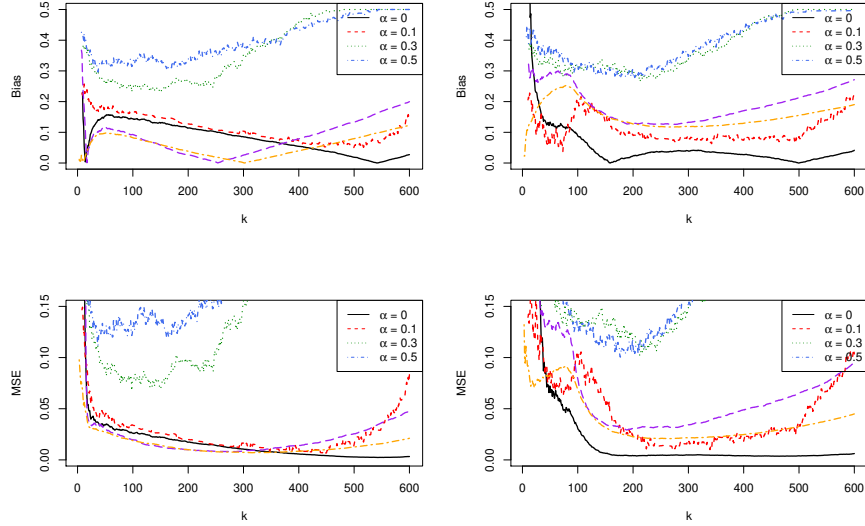


FIGURE 9.15. Bias (top panel) and MSE (bottom panel) of the MDPD tail index estimator  $\hat{\gamma}_{1,\alpha}$ , together with  $\hat{\gamma}_1^{(EFG)}$  (long-dashed purple line) and  $\hat{\gamma}_1^{(W)}$  (two-dashed orange line) computed from 2000 Monte Carlo samples of size 1000 generated from Scenario **S2**, with  $\gamma_1 = 0.5$ ,  $\gamma_c = 0.8$  and  $p = 0.55$ . Contamination is introduced after the censoring mechanism, with  $\epsilon = 0$  (left panel),  $\epsilon = 0.15$  (middle panel), and  $\epsilon = 0.40$  (right panel).

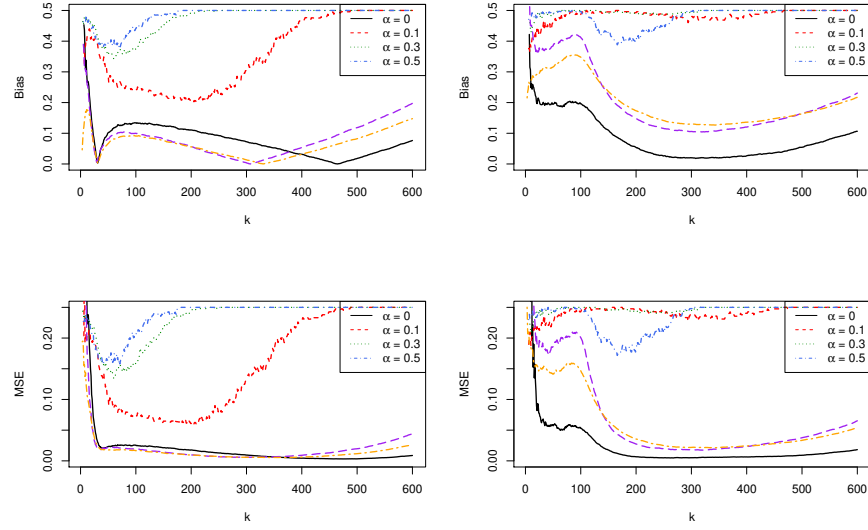


FIGURE 9.16. Bias (top panel) and MSE (bottom panel) of the MDPD tail index estimator  $\hat{\gamma}_{1,\alpha}$ , together with  $\hat{\gamma}_1^{(EFG)}$  (long-dashed purple line) and  $\hat{\gamma}_1^{(W)}$  (two-dashed orange line) computed from 2000 Monte Carlo samples of size 1000 generated from Scenario **S2**, with  $\gamma_1 = 0.5$ ,  $\gamma_c = 0.8$  and  $p = 0.7$ . Contamination is introduced after the censoring mechanism, with  $\epsilon = 0$  (left panel),  $\epsilon = 0.15$  (middle panel), and  $\epsilon = 0.40$  (right panel).